August 2020

Optimizing Energy Savings for a Fleet of Commercial Autonomous Vehicles via Centralized and Decentralized Platooning Decisions

Dahui Liu
Clemson University, ldhkevin0926@gmail.com

Optimizing Energy Savings for a Fleet of Commercial Autonomous Vehicles via Centralized and Decentralized Platooning Decisions

---

A Dissertation
Presented to
the Graduate School of
Clemson University

In Partial Fulfillment
of the Requirements for the Degree
Doctor of Philosophy
Industrial Engineering

---

by
Dahui Liu
August 2020

Accepted by:
Dr. Amin Khademi, Committee Chair
Dr. Burak Eksioglu
Dr. Sandra Eksioglu
Dr. Mashrur Chowdhury
Dr. Tugce Isik

Abstract

Thanks to advanced technologies like Connected and Autonomous Vehicles, platooning is becoming more and more useful as a method to potentially increase road capacity and reduce energy consumption. While there are many studies in the literature reporting significant fuel and energy savings as a result of platooning, these studies are ignoring the extra energy required to maintain vehicles in close formation referred to as string stability. Also, there are other factors many of the current studies are not considering such as the position of a vehicle in a platoon, the background traffic that may complicate the process of forming platoons, and the vehicle type. Thus, optimizing and quantifying the savings that may be gained from platooning is challenging. In this study, we develop a simulation-optimization framework to tackle this challenge. The simulation model simulates real traffic conditions for individual vehicles and platoons. Additionally, the simulation model implements platoon forming decisions obtained from an optimization model. Vissim is used to simulate the actions taken by all the vehicles and platoons and capture the energy expended by each vehicle over its entire trip duration. Our optimization model determines vehicle-to-platoon assignments given the locations, speed, and acceleration of vehicles and platoons. Particularly, we concentrate two different optimization models. One is a centralized model to make platooning decisions with aim to maximize potential energy savings system-wide. On the other hand, a decentralized model utilizing a competition game is developed to make decisions for individual vehicle energy saving purpose. In addition to the simulation-optimization framework, an accurate energy consumption model is developed, which is inspired by the work of Tadakuma and colleagues. The energy consumption model utilizes a hybrid prediction formula for aerodynamic drag reduction in multi-vehicle formations unifying both physical mechanisms and existing empirical study data. In addition to the centralized and decentralized decision making models, we track a single platoon to observe the energy consumption for this one platoon under different parameters in order to better understand the factors that impact energy savings. Our results show that a system-wide savings of about 3% in centralized model, and 1.5% in decentralized model can be realized over 100 miles when platoons are

formed strategically. Comparison between two models also confirm, as expected, that the centralized model forms better platoons in terms of energy savings.

Acknowledgments

I would like to greatly thank my supervisor, Burak Eksioglu, for his instruction, guidance, support, and patience. Without him I would not have been able to complete my research and improve my research skills.

I would like to thank following professors in my research group who have helped me conduct this research. Dr. Matthias Schmid, for his support and encouragement, especially contributions to energy model in our project. Dr. Nathan Huynh, for his help, patience, and many valuable advice for our project. Dr. Gurcan Comert, for his enthusiastic and assistance on Vissim application.

I would like to acknowledge the Center for Connected Multimodal Mobility (C^2M^2), for funding this project.

I would also like to thank my committee members, Dr. Amin Khademi, Dr. Sandra Eksioglu, Dr. Mashrur Chowdhury and Dr. Tugce Isik, for their guidance during the entire period I am working for my PhD.

Table of Contents

List of Tables

List of Figures

Chapter 1

Introduction

As Intelligent Transportation Systems (ITS) and Connected and Autonomous Vehicles (CAVs) are becoming more and more advanced, vehicle platooning could potentially become a reality in the near future. A platoon is a fleet of vehicles that travel together at the same speed with uniform short following inter-vehicle space. With short following distances, both front vehicle and following vehicle can obtain air drag reduction benefits which in turn reduce energy to move these vehicles. In addition, short following distances potentially increase traffic throughput. On the other hand, however, vehicles may consume more energy as they accelerate or decelerate to form platoons. In addition, it is impractical to have a large number of vehicles in each platoon due to safety, control issues, locally congestion, and not providing sufficient space for vehicles in adjacent lanes to switch lanes. Hence, we would like to study the practical benefits of platooning.

1.1 Overview of this study

In this paper, we mainly investigate the effect of platooning on energy consumption for a fleet of connected and autonomous trucks traveling over a long freeway stretch with on- and off-ramps. Two type of formulations are used to make platooning decisions. For centralized model, given the destination for each vehicle in the system, the target is to identify best possible opportunities for entire system such that individual CAVs can dynamically join and leave platoons. Unlike the centralized model, decentralized formulation find best strategies for locally single vehicles. Thus, so as to optimize and quantify the potential savings, a simulation-optimization framework is built in this study. In this framework, the optimization model forms platoons with different approaches and the simulation model captures the realistic vehicle movements, traffic

conditions, and energy consumption. A comparison between two optimization models is conducted in this study to evaluate the effectiveness of these two models.

In order to obtain more precisely energy consumption information, we develop a prediction energy consumption model in this study. In addition, we focus on energy consumption instead of fuel consumption since energy consumption eliminates the need to specify engine types for various vehicles. In other words, energy consumption and fuel consumption are closely related, but the latter depends on the specifications of the engine on each vehicle. Fuel consumption can be calculated according to energy consumption and engine type. Existing research either focuses on assessing aerodynamic forces through simulation, scaled testing in wind tunnels, or limited full-scale track testing by involving the use of actual vehicles, pressure sensors to measure drag, and scales to measure the change in fuel (*e.g.*, [1]–[5]). To date, models to predict energy consumption of vehicles in a platoon traveling at the same speed with very short inter-vehicle distances are limited. These types of models are of paramount importance for cooperative adaptive cruise control (CACC) applications. Our prediction energy consumption model fulfills this gap in the literature by proposing a model that combines empirical data and physics-based modeling.

Additionally, we observe the energy consumption of one selected platoon driving through this entire freeway. Several experiments are conducted with different factors such as desired travel speed, inter-vehicle distances, platoon size. Meanwhile, data is recorded to analyze the energy situation of that platoon. With results, we better understand energy composition for an individual platoon.

The remainder of the research is organized as follows. In 1.2, we provide a brief review of the literature related to optimization, simulation, and energy models for platooning. Chapter 2 provides details of our simulation-optimization approach and our energy consumption model. In particular, section 2.1 introduces simulation-optimization framework. Simulation and network settings are present in section 2.2. In addition, sections 2.3 and 2.4 states our prediction energy model and results. Chapters 3 and 4 detailed present our centralized and decentralized formulations with experiments and results respectively. With similar format, sections 3.1 and 4.1 present a linear programming model (centralized) and a dynamic game model (decentralized). Sections 3.2, 3.3, and 3.4 show experiments, traffic condition results, and energy consumption results for centralized model. Same as sections 4.2, 3.3, and 4.4 for decentralized model. Moreover, information and analysis of that one platoon observed is shown in chapter 5. Lastly, comparison, evaluation and conclusion are provide in chapter 6, including a detailed analysis of the difference of two models in section 6.1, and conclusions with future research.

1.2 Literature Review

Vehicle platooning is not a new concept. Researchers have been investigating platooning since the early 1950s. However, due to the technology of the time, these research efforts were mostly theoretical without any real-life applications. In recent years, more project were conducted to research platooning method. From mid 1990s to early 2000s, the "Chauffeur" group within the European Union (EU) project T-TAP ([6], [7]) studied automation in trucks. A longitudinal control concept and a two layered control structure were established for controlling platoons. An experiment was created with three vehicles travelling along the Brenner Pass as a platoon for field test. From 2005 to 2009, the German project KONVOI conducted a study on a platoon of four trucks [8]. The platoon drove on German highways (lead vehicle was driven by a human driver) with a gap of 10 meters (m) between vehicles. They reported an increase of up to 9% in road capacity and a decrease of up to 10% in fuel consumption. The Japanese project "Energy ITS" starting in 2008 built a platoon of 3 heavy trucks and 1 light truck with a gap of $4.7m$ between and an average speed of 80 kilometer per hour (kph) [9]. The project reported a 15% savings in fuel consumption based on their field experiments. In addition, they also concluded that a 40% penetration in heavy trucks can result in 2.1% CO_2 emission reduction with a gap of $10m$ in a simulation study. In 2011, the California PATH program conducted a test with a platoon of three trucks at a gap of $6m$ [10]. The results showed an average of 4-5% fuel savings for the lead truck and 10-14% for the following trucks.

As known in theory of aerodynamic, platooning can reduce energy consumption primarily due to changes in aerodynamics. As can be seen in Figure 1.1, air drag reduction mainly depends on inter-vehicle distance and position in platoon. While not shown in Figure 1.1, air drag reduction also depends on the speed at which the platoon is traveling. Other research studies confirm these observations. For example, Browand *et al.* [11] report fuel savings of 8-11% for a platoon with two trucks. Bonnet and Fritz [2] study a platoon of two trucks travelling at 60 kph and $80kph$ on a highway with additional traffic. They show that the decrease in fuel consumption ranged from 15% to 21% at $80kph$ and 10% to 17% at $60kph$ for the tail truck, and 3-10% at $80kph$ and 3-7% at $60kph$ for the lead truck. Tsugawa [12] shows a 14% decrease in fuel consumption in a study with three trucks driving at $80kph$ with $10m$ inter-vehicle gaps. Lammert *et al.* [3] provided experiments and statistical analyses for platoons with different inter-vehicular distances, speeds, and masses. The paper provided a range of 3-9% fuel reduction for tail trucks and 2.5-5.5% for lead trucks.

With respect to quantifying vehicle fuel consumption, majority of the models are either statistical or physical. Statistical models establish a relationship between vehicle system inputs and fuel consumption. The

consumption is usually estimated every second, which requires input data at the same time resolution. Barth *et al.* [14] were the first to build a linear regression model to estimate energy consumption and emissions of vehicles based on engine output power. Later, Rakha *et al.* [15] developed the VT-Micro model, which estimates fuel consumption based on a vehicle's second-by-second travel speed and acceleration. Physics-based models, on the other hand, simulate the physical powertrain working processes to quantify fuel consumption. FASTSim, used in a study by Brooker *et al.* [16], and autonomy, used in a study by Halbach *et al.* [17], are examples of physics-based models. Since these models are based on physical simulations, the drag coefficient is included as an influencing factor that determines energy consumption. Some studies (*e.g.*, [18], [19]) have utilized physical models to assess energy consumption of many driving cycles. The physics-based approach provides the flexibility to comprehensively examine the effects of inter-vehicle distance, speed, vehicle type, and other factors on fuel savings. One of the major factors that significantly affects a vehicle's fuel savings is its coefficient of drag. Hence, Tadakuma *et al.* [20] establish a prediction formula for estimating aerodynamic drag reduction which considers different vehicles types and inter-vehicle distances. Based on their model, a hybrid prediction formula is provided for energy calculation.

In addition to the energy studies provided above, there are also some optimization and simulation studies on fuel/energy savings. Tsugawa *et al.* [21] developed a computational fluid dynamics (CFD) simulation with a platoon of three vehicles traveling at 80kph with an inter-vehicle gap of 4m. Their results show that all three trucks consumed less fuel compared to when they were traveling singly, but the middle truck

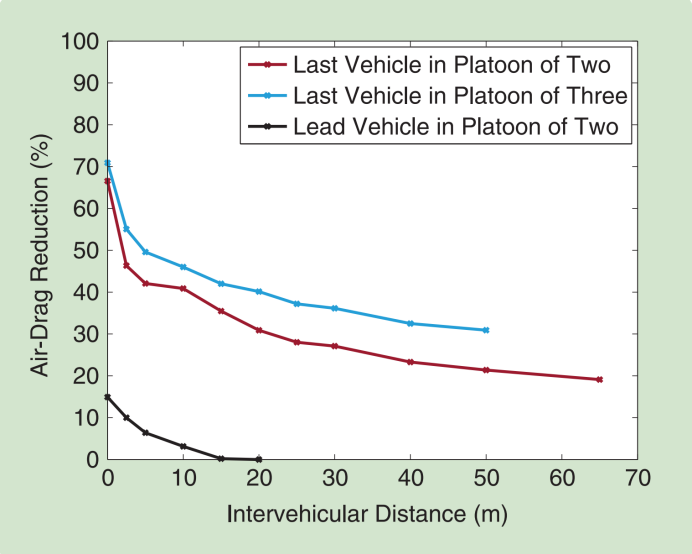

Figure 1.1: Air drag reduction for buses in a platoon at 80kph (Source: [13])

had the highest fuel savings. Deng [22] provided a simulation framework for a platoon with two vehicles to study different platoon forming methodologies and concluded that platooning can improve traffic flows. Johansson [23] developed a speed control approach to maximize fuel savings and used a simulation model to test fuel consumption, throughput, and safety where safety issues mainly depend on acceleration distribution and time gaps to front vehicles. Optimal deceleration trajectories are used in their simulation to avoid crashes. The above mentioned papers focus on controlling existing platoons (not forming new platoons) in real traffic conditions to optimize fuel consumption or flow capacity. On the other hand, Heinovski and Dressler [24] set up centralized and distributed approaches to optimize travel time and fuel efficiency of platoons based on their desired speed and current position. Larson *et al.* [25] developed a distributed method for optimizing platoon routing with a local controller. Their work focuses on speed control, and they do not consider the position of the vehicles in a platoon. In a similar study, Liang *et al.* [26] develop an optimization model for two vehicle formations. Dao *et al.* [27], [28] studied a platooning problem similar to ours. They provided an optimization-simulation model in which the objective function is to maximize the total distance that platoons stay intact with the aim to improve lane throughput.

In terms of using decentralized model in platooning problem, several studies concentrate on setting up decentralized control schemes. For examples, Han *et al.* [29] established a longitudinal tracking control law for Cooperative Adaptive Cruise Control (CACC) to improve safety with capability of tracking inter-vehicle spacing, velocity and acceleration. Renzler *et al.* [30] provide decentralized dynamic platooning architecture to maintain safety based on network reliability, environmental. In addition, Rupp *et al.* [31] and Kumaravel *et al.* [32] study a merging problem of vehicles and platoons on changing from two lanes to one lane. Rupp *et al.* [31] establish a decentralized cooperative algorithm for vehicles to merge lane safely with shorter inter-vehicle distance. While Kumaravel *et al.* [32] provide a optimal schedule and a decentralized control algorithms for cooperative merging of platoons at freeway on-ramps. Refer to game theory in platooning problem, there are plenty of games are used in different area of platooning. For examples, Sajjad *et al.* [33] formulate a zero-sum game to determine the optimal strategy of attackers and defenders, who try to disrupt or maintain the operation of platoon respectively. Gattami *et al.* [34] study a safety problem of heavy duty vehicle platooning. A pursuit-evasion game is built in their model to set safety criteria for heavy duty vehicle. They conclude a minimum $1.2m$ inter-vehicle distance without causing collision. Moreover, Farokhi and Johansson [35] develop an atomic congestion game with cars and trucks as players. In their research, car only considers own benefits such as preferred time, traffic flow velocity, and congestion penalty, while trucks also consider platooning benefit such as fuel efficiency. Johansson *et al.* [36] and Johansson and

Mårtensson [37] formulate a games of platoon matching problem. Trucks as players with same origin, but different destinations want to departure at the same time to benefit from platooning, but not cost more.

Based on this review of the relevant literature, it is evident that a study is needed to look at system-wide improvement opportunities under developing CAVs framework. Building an centralized optimization system-wide can potentially yield to great savings. However, considering a large system, sometimes, it may be difficult to optimize and make decisions through a centralized horizon. Although centralized decision model can provide better results, the cost to make decisions, such as information sharing, information collection, and time to obtain optimal solution, may not acceptable. Therefore, a decentralized model should be considered based on locally information set as well. In addition, better platoon forming and maintaining method can reduce energy waste due to acceleration. Thus, in our study, we mainly focus on (1) optimizing energy savings system-wide via centralized decisions to form platoons (2) optimizing potential energy savings for each individual vehicles via decentralized game formation, (3) simulating the traffic stream that consists of platoons and individual vehicles from the microscopic simulation model, (4) determining actual energy consumption based on our prediction energy model, and (5) comparing differences of results between centralized optimization and decentralized strategic game. (6) Energy consumed of that observed platoon is also be analyzed.

Chapter 2

Research Design and Methods

In this chapter, we detailed present the simulation-optimization framework as our primary research design. Systematically, whether centralized, decentralized model, or the observation of one picked platoon is based on the interaction in simulation-optimization framework. In addition, specific simulation environments and settings are introduced here. Note that, all experiments utilize this presented simulation model with same or similar parameters in order to conduct fair comparison and analysis. Since different formulations in this research concentrate on energy consumption, prediction energy consumption model is elaborate presented too.

2.1 Simulation-Optimization Framework

We develop a simulation-optimization framework to quantify the potential energy savings for a fleet of autonomous trucks as they travel on a long highway stretch. This framework contains two major parts, simulation model and optimization model. More specifically, a microscopic simulation model is set up that realistically simulates the movements of this fleet of vehicles and other traffic status of vehicles on the freeway. The optimization model, from another point of view, partitions the traffic network into platooning zones around each on- and off-ramp. For each zone created, the model finds the best possible assignment of each single vehicle to a platoon by considering either whole shared information set or some locally limited information set. There is a feedback loop between the simulation and optimization models. In other words, two models interact with each other in order to provide precise information of platooning utilizing in real traffic. Figure 2.1 below provides a flow chart showing how the optimization and simulation models interact.

As can be seen in Figure 2.1, we simulate the system for T periods. The optimization model is run every τ period. Each time the optimization model is run, single vehicles are potentially assigned to nearby platoons according to decisions made in centralized or decentralized model. The simulation model takes these platooning decisions as input and simulates the traffic until the next optimization period. In the mean time, traffic situation changes continuously such that new vehicles may enter the highway and some vehicles may reach their destinations. This dynamic process is repeated until the end of the planning horizon at which point system performance measures are collected.

2.2 Simulation Model

Vissim (`http://vision-traffic.ptvgroup.com/en-us/products/ptv-Vissim/`), a microscopic simulation environment, is utilized to generate the network and simulate the traffic. Thus, our simulation model is established in Vissim. In terms of traffic network and vehicles settings, mainly, the default settings were adopted in Vissim. The COM interface via Python scripts are used to manage the platoons. The following sections provide more details about the settings.

2.2.1 Vehicle and network settings

Since the main objective of this study is to quantify energy savings via platooning, we created a 100-mile highway stretch in Vissim as our basic network framework. This highway stretch is designed as a

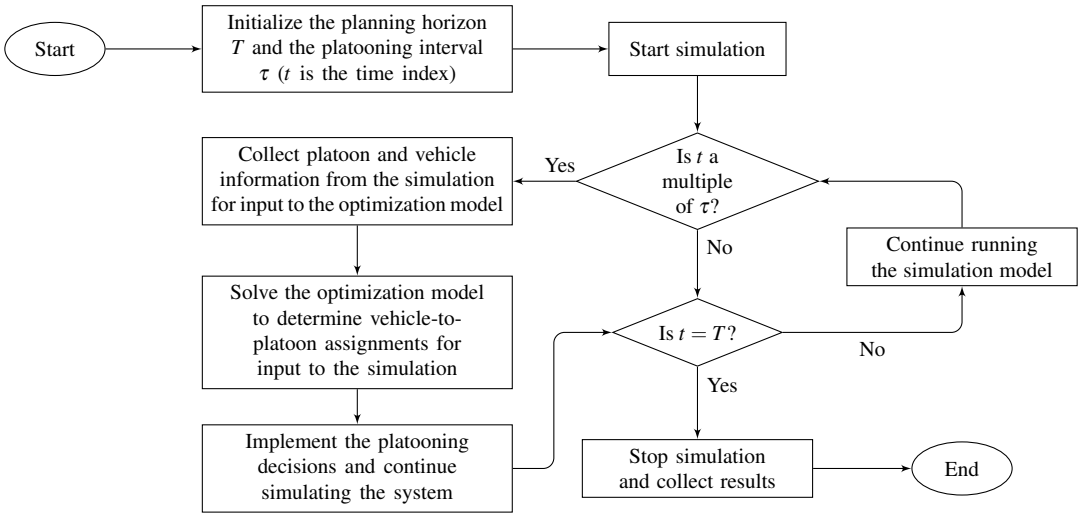

Figure 2.1: Flow chart of the simulation-optimization framework

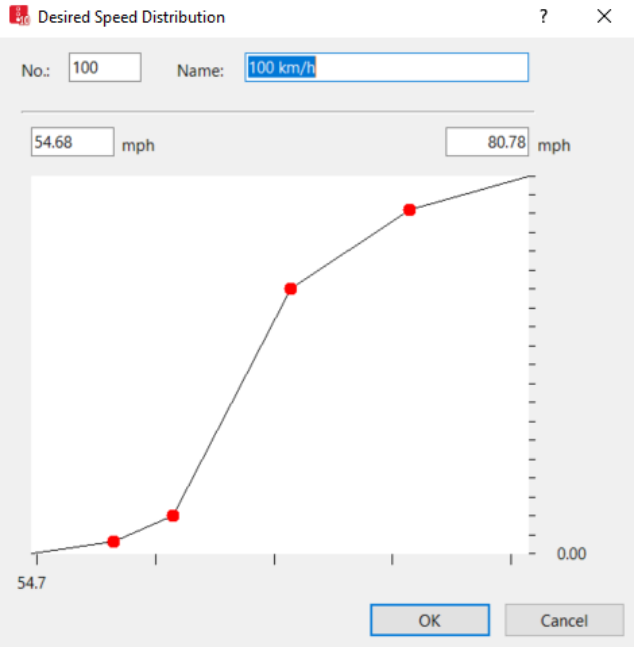

Figure 2.2: Desired speed distribution

level terrain with no curves, and has three lanes in the same direction. We will refer the right lane as Lane 1, the middle lane as Lane 2, and the left lane as Lane 3 throughout the paper. There are 36 on- and 36 off-ramps distributed almost evenly over this highway stretch. The default freeway settings are applied (*e.g.*, $12ft$ lane width) in Vissim. All vehicles, entering the highway individually or in a platoon, are Heavy Goods Vehicles (HGVs), where single vehicles follow a desired speed distribution in Vissim (shown in Figure 2.2) with an average of 62.5 miles per hour (mph) or $100kph$.

In this network, platoons are allowed only in Lanes 2 and 3 for the reason that, in our preliminary simulations, allowing platoon to travel in Lane 1 led to heavy congestion and traffic jams. From a practical perspective, it is also a reasonable assumption, since allowing platoons in Lane 1 would impact the entry and exit of vehicles from the ramps. Unlike the single vehicles, desired speed of platoons are fix. The desired speed of the platoons in Lane 3 is set to $65mph$ and those in Lane 2 is set to $60mph$ or $55mph$ based on different experiments. The Vissim screenshots in Figure 2.3 show the driving behaviour settings. As can be seen from Figure 2.3, the HGVs in a platoon drive at close inter-distance (*i.e.*, 0.5 second (s) time headway).

Similar to the network settings, we use the default Vissim values for many of the vehicle characteristics. For example, the length and the width of the HGVs in our system are $33.51ft$ and $8.19ft$, respectively. We also use the default acceleration, deceleration and other parameters for the HGVs. Figure 2.4 shows the

distributions for the desired and maximum acceleration for the HGVs in which the x-axis and y-axis represent speed (mph) and acceleration (ft/s^2), respectively. In these figures, the middle curve (with red dots) shows the mean acceleration values at different speeds. The curve above (below) the middle one shows the maximum (minimum) acceleration values. We enforce these upper and lower bounds so that the vehicles are not using unrealistic accelerations. Another factor in energy consumption is the weight of the vehicle. We used the mean total vehicle weights from two published reports ([38], [39]) in our simulations.

2.2.2 Vehicle and platoon control methods

In the simulation, platoons enter the highway at mile zero every 60s for each lane. The first platoon in Lane 3 is generated as soon as the simulation begins, while the first platoon in Lane 2 enters after 30s. Hence, platoons enter this highway in turn from Lane 3 and Lane 2. Platoon sizes are generated uniformly between 2 and 5 vehicles and the headway between vehicles is set to 0.5s for both control and energy savings proposes. Each vehicle (single or in a platoon) is randomly assigned a destination once it enters the highway. In our initial set of experiments, vehicles pick remaining off-ramps as destinations based on a uniform distribution, which led to extreme congestion especially in the latter of freeway. To eliminate this problem, we experimented with several different distributions before finally developing a probability mass function that

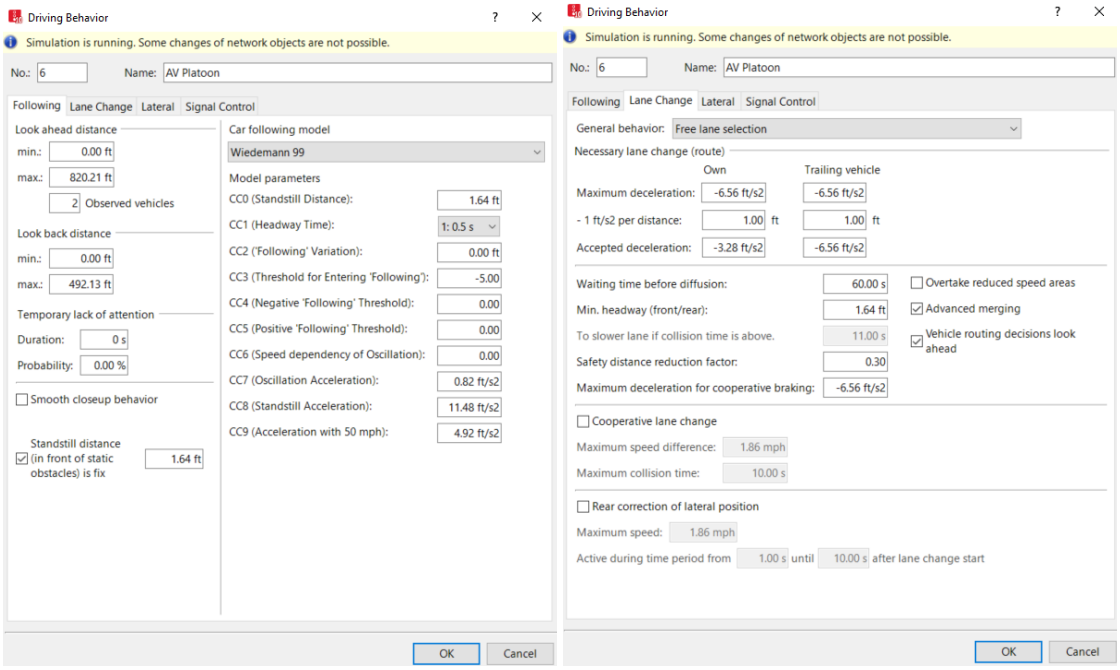

Figure 2.3: Following and lane changing behavior

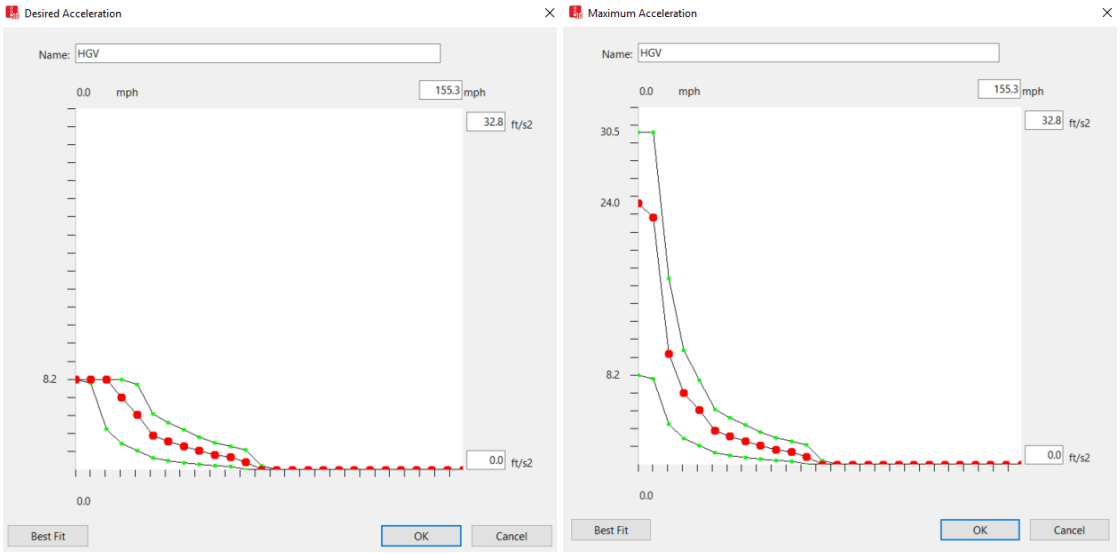

Figure 2.4: Desired and maximum acceleration distributions in Vissim

resembles a geometric distribution.

Let $N_D - 1$ be the number of off-ramps in the network after the on-ramp from which a vehicle enters the highway. This vehicle will exit the system either from one of these off-ramps or the end of the highway. Thus, there are N_D potential destinations for the vehicle. For a vehicle that enters the highway from mile zero all 36 off-ramps and the end of the highway are potential destinations, *i.e.*, $N_D = 37$. On the other extreme, for a vehicle that enters the highway from the last on-ramp $N_D = 1$. Our function of geometric distribution ensures that vehicles do not leave the highway too soon (*i.e.*, they get an opportunity to join a platoon), and they do not stay too long to cause congestion. Let p_l ($l = 1, 2, \ldots, N_D$) be the probability that potential destination l is assigned as the final destination for this vehicle. The probability mass function developed is as follows:

$$p_1 = \frac{\rho(1+\rho)^{N_D-3}}{(1+\rho)^{N_D}-1}, \quad p_3 = \frac{\rho(1+\rho)^{N_D-1}}{(1+\rho)^{N_D}-1}, \tag{2.1}$$

$$p_l = \frac{\rho(1+\rho)^{N_D-l}}{(1+\rho)^{N_D}-1}, \qquad l = 2, 4, 5, \ldots, N_D \tag{2.2}$$

where $0 < \rho < 1$ is the shape parameter. After experimentation with different values, $\rho = 0.2$ was chosen as it resulted in stable traffic flow with opportunities for platooning. Figure 2.5 shows the probability mass function when $N_D = 10$. As shown in this figure, it does not look like a geometric shape since we switch the probability of the first and the third possible exits in original geometric distribution so as not to encourage

vehicles leave too soon. In addition, far destinations have small probabilities to ensure more stable traffic flow.

To minimize energy consumption due to acceleration of platoons and single vehicles, we only allow single vehicles to join platoons that are behind them. Thus, in our optimization model, for each single vehicle in a platooning zone only those platoons that are behind the vehicle are considered. Once the optimization model determines which platoon a particular vehicle needs to join, that vehicle moves to Lane 1 and slows down to 40mph. We make single vehicles adjust their speed instead of platoons due to the reason that platoons will consume more energy by changing speed comparing an individual vehicle. When the platoon is within a certain distance (S_0) of the vehicle then the vehicle starts to speed up and move to Lane 2 or 3 depending on where the platoon is. On one hand we want the single vehicle to join the platoon as soon as possible so that it can travel with the platoon for a longer period of time. On the other hand, however, we don't want the vehicle's acceleration to be too high during this joining process because that will increase its energy consumption. To ensure a smooth joining process we use the following process and the equations:

$$\begin{cases} v_j = v_i + at, \\ v_j t = v_i t + \frac{1}{2} a t^2 + S_0 \ . \end{cases}$$

Assume that platoon j and single vehicle i will merge in Lane 3. This means the desired speed of the platoon is 65mph (v_j=65). Recall that the desired speed of the single vehicle is initially 40mph (v_i=40).

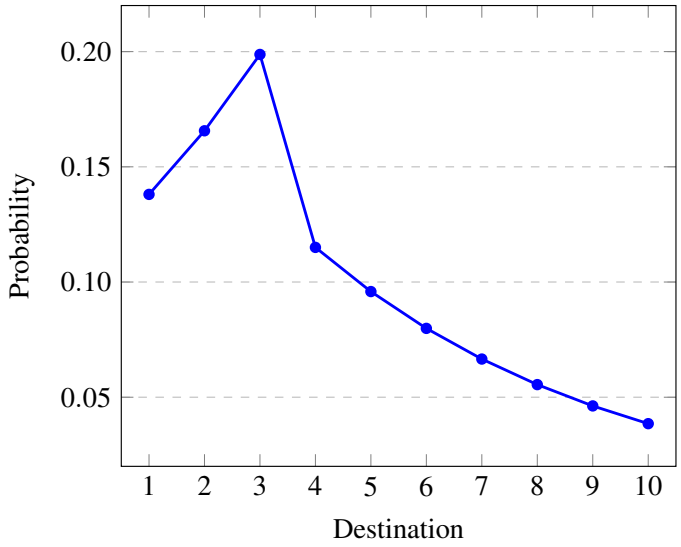

Figure 2.5: Probability mass function when $N_D = 10$

Vissim determines the acceleration of the vehicle using the distribution given in Figure 2.4. In terms of this distribution, an average acceleration (a) is calculated for that v_i. Now, using the first equation above, we can calculate the time (t) it will take v_i to increase to 65 with acceleration (a). Then, using the second equation we can calculate S_0. Thus, when platoon j is within S_0 feet of vehicle i then v_i is increased by $5mph$. Since acceleration picked from distribution may larger or smaller than average, it may take different time to reach new v_i. Then, we use the new value of v_i and average acceleration a for new v_i to calculate a new t value and eventually a new S_0 value. The advantages of increasing speed step by step ($5mph$) are to make Vissim pick another acceleration in order to avoid too bad choice. This process of increasing v_i is repeated until the vehicle joins the platoon.

As mentioned above, to minimize energy consumption, each platoon should ideally travel at a constant speed (*i.e.*, avoid accelerating or decelerating). However, this is not an easy task even in a simulation. One of the things we implemented is to enforce the platoons to stay in the same lane. Individual vehicles change lanes to join or leave a platoon, but platoons are forced to stay in their lanes. Also, we assume that the HGVs in our fleet have cooperative adaptive cruise control (CACC). This allows us to have the vehicles travel at closer inter-vehicle distances. Yet, each vehicle in the platoon still has to accelerate or decelerate to maintain the $0.5s$ headway. In particular, when a vehicle approaches its destination it begins to move to Lane 1 and get ready to leave the highway. The other vehicles (if any) in the platoon that are behind the leaving vehicle begin to accelerate to close the gap. When vehicles accelerate or decelerate Vissim determines the exact value based on the distributions shown in Figure 2.4.

2.3 Prediction Energy Consumption Formulation

Energy consumption depends on many factors such as speed, acceleration, mass, gradient, road condition, wind, and frontal area of the vehicle. We focus on three important energy consumption areas that account for the main difference between vehicles traveling singly or in a platoon: (*i*) acceleration, (*ii*) rolling friction, and (*iii*) aerodynamic drag.

The total energy consumed in truck platooning is usually reported in terms of fuel consumption. Yet, the operating fuel consumption of a vehicle depends on a multitude of factors, *i.e.*, the efficiency of the engine, transmission characteristics, weight of the vehicle, aerodynamic resistance, rolling resistance of the tires, driving cycle, and driver behavior [40]. While engine and transmission losses are significant, they can be represented in the simplified form of a constant scaling factor (for driving with or without platooning).

Hence, this study focuses only on the energy necessary to physically move a vehicle, which can be converted to fuel consumption. The forces which need to be overcome to maintain a constant speed, *i.e.*, the road load, yield

$$\begin{aligned} R(t) \;&=\; [mg\,\cos(\alpha) - F_L] \cdot \left(f_0 + k_R\, v(t)^2\right) \\ &+\; F_D \;+ mg\,\sin(\alpha) \end{aligned} \tag{2.3}$$

with m and g being the mass and the gravitational constant, α representing the grade of the road, F_L denoting the aerodynamic lift force, f_0 and k_R being constant and velocity dependent rolling resistance coefficients, and F_D designating the aerodynamic drag. For heavy-duty vehicles, the effect of aerodynamic lift on the rolling resistance can be neglected. As the goal of this study is to provide a drag reduction ratio (DRR) prediction (and subsequently an energy reduction rate) for platooning operations, the development of this ratio will be independent of the road grade. It is therefore acceptable, without loss of generality, to limit the analysis to a level road. Hence, the vehicle specific power ([41]) reduces to

$$\begin{aligned} VSP \;&=\; [R(t) \;+\; m\,a(t)] \cdot\; v(t) \\ &=\; \left[f_0 + k_R\, v(t)^2\right] \cdot v(t) + m\,a(t)\;\cdot v(t) + \;F_D \cdot v(t). \end{aligned} \tag{2.4}$$

Here, $v(t)$ is the instantaneous speed at time t and $a(t)$ the instantaneous acceleration. As the promised fuel savings in platoon operations arise from reduced aerodynamic drag, the following sections will detail the methodology to arrive at a hybrid prediction formula for the DRR. This equation includes energy from rolling friction (first term), energy from acceleration (second term), and energy from drag reduction (third term) as we mentioned.

The terms for energy from rolling friction and acceleration are straight forward. However, energy savings from drag reduction are complex. To supply an assessment model for drag coefficient reduction, this part modifies the prediction formulas developed by Tadakuma *et al.* [20] and adapts them to experimental data for heavy-duty vehicles. In order to maintain consistency of the prediction model for long, medium, and short inter-vehicle distances, several phenomena must be included: reduction of the main flow velocity in a vehicle's wake, stagnation pressure created in front of a follower vehicle as well as behind a leading vehicle, nonuniformity of flow at short distances, and unmodeled effects for long platoons. We partially utilize functional forms from [20] while expanding the relationship for stagnation pressure and introducing

a concatenation correction. The introduced shift parameter effectively removes the previous unrealistically high reduction in aerodynamic drag for short distances while the concatenation term allows for omitting the nonuniform flow correction. For parameter estimation and fitting of the physical model to data from heavy-duty truck testing, a least squares regression is employed.

In general, the force resulting from aerodynamic drag in the context of single vehicle driving is expressed via the following relationship:

$$F_D = \frac{1}{2} \cdot \rho \cdot C_D \cdot A_f \cdot v(t)^2. \tag{2.5}$$

Here, ρ denotes the density of air, C_D the drag coefficient, A_f the total projected frontal area, and $v(t)$ the velocity of the vehicle. The utilization of the drag coefficient - reflecting the aerodynamic behavior resulting from the shape of the vehicle - allows for this simplified representation. Additionally, the drag coefficient for a given vehicle can be easily obtained experimentally (*e.g.*, in a wind tunnel) by measuring the perceived drag force for a given air velocity. As Eq. (2.5) only holds for single vehicle driving, the travel velocity coincides with the air velocity received by the frontal area of the vehicle. This will, in general, not be true for vehicles driving in a platoon. Furthermore, Eq. (2.5) is subject to additional assumptions: (*i*) uniform flow; (*ii*) no atmospheric wind; and (*iii*) no skin friction. All employed coefficients of drag within this study should be interpreted as coefficients of pressure drag.

With the goal of a hybrid expression for fuel savings in mind, the role of aerodynamics under platooning can be expressed by comparing pressure drag between solo driving, F_{Ds}, and platooning, F_{Dp}, to arrive at the DRR, *i.e.*,

$$\begin{aligned} DRR &= \frac{F_{Ds} - F_{Dp}}{F_{Ds}} \\ &= \frac{C_{Ds} \cdot A_f \cdot q_s - C_{Dp} \cdot A_f \cdot q_p}{C_{D,s} \cdot A_f \cdot q_s} \\ &= 1 - \left[\frac{q_p}{q_s} \cdot \frac{C_{Dp}}{C_{Ds}} \right]. \end{aligned} \tag{2.6}$$

Here, the dynamic pressures (velocity pressures) received at the frontal area of the vehicle under solo driving and under platoon driving, q_s and q_p, are utilized instead of the vehicle velocity v as $q = \frac{1}{2}\rho u^2$ for compressible fluids at low Mach numbers (with u being the flow speed). Note that this ratio will be 1 for the first vehicle. The dynamic pressure ratio q_p/q_s as well as the uniform flow equivalent drag coefficient under platooning C_{Dp} need to be determined by including correction terms for four distinct effects apparent for each

vehicle in the interior of the platoon:

1. The wake of a leading vehicle reduces the main flow velocity and, thereby, the dynamic pressure received by a follower. This phenomenon can be expressed via the ratio of the center line air velocities for a vehicle in the wake and solo driving, u_w/u_s. This effect appears over a wide range of distances (long, medium, and short).

2. For short inter-vehicle distances, stagnation pressure is created in the front of the ego vehicle (if the ego vehicle is not the lead vehicle of the platoon). The increase of pressure over the frontal area raises the main flow velocity again, thereby adversely affecting the ratio of the center line velocities u_w/u_s. Thus, a correction factor for the previous wake velocity deficiency needs to be introduced.

3. On the other hand, stagnation pressure is also created by a follower vehicle at the rear base of the ego vehicle for short distances in a platoon. This rear base pressure lowers the pressure drop over the body of the ego vehicle, and thus, the flow. Hence, another correction term reflecting this effect is needed for the drag coefficient C_{Dp}. In contrast to the stagnation pressure created in the frontal area of the ego vehicle, this phenomenon yields a pushing effect, *i.e.*, increases DRR.

4. The expression in Eq. (2.5) inherently assumes uniform flow to allow for the simplifying use of the drag coefficient C_D. However, if inter-vehicle distances in a platoon are short to medium, nonuniform flow effects arise. Therefore, Tadakuma *et al.* introduced a flow correction term in the modified drag coefficient C_{Dp} in [20]. As will be specified later, our approach does not necessitate this correction term, but requires a concatenation factor for long platoons, *i.e.*, those with 3 or more vehicles.

Stagnation Pressure: The stagnation pressure created at the base of the ego vehicles by a following vehicle leads to a pushing effect reflected in a decrease of the drag coefficient under platooning. This is the only platooning impact apparent for the lead vehicle. Tadakuma *et al.* [20] introduce an analytical expression for the base pressure of the i^{th} vehicle that is "based on a formula that expresses the changes in the coefficient of pressure caused by a potential flow" as

$$\frac{\Delta C_{Db,i}}{C_{Ds,i}} = 1 - \left[1 - \left[\frac{\varepsilon}{d_{i(i+1)}+\varepsilon}\right]^3\right]^2. \tag{2.7}$$

Here, ε is an empirically established constant (determined as $\varepsilon = 6.3$ for sedan-type vehicles), whereas $d_{i(i+1)}$ is the distance between vehicles at positions i and $(i+1)$ in the platoon. However, the reasoning for this

expression cannot be confirmed as the referenced work in [20] is only available in Japanese. Additionally, the functional form of Eq. (2.7) requires adjustments when used to assess the fuel saving benefits of platooning at small inter-vehicle distances: $\Delta C_{Db}/C_{Ds}$ approaches 1 for $d_{i(i+1)}$ going to 0, *i.e.*, the lead vehicle in the platoon will have no drag for very small distances. This does not correspond to physical reality. Especially for the small inter-vehicular distances to be exploited in platooning when utilizing CACC, the expression in Eq. (2.7) becomes highly erroneous and over-promises fuel savings. This is one of the reasons that the prediction formula in [20] fails to follow the trend of the empirical data obtained, for instance, by McAuliffe *et al.* [1]. Hence, we suggest a new functional form for the stagnation pressure correction that maintains a hyperbolic character, but introduces a second parameter for horizontal shift. This new expression does not exhibit a singularity at $d_{i(i+1)} = 0$ and yields

$$\frac{\Delta C_{Db,i}}{C_{Ds,i}} = 1 - \left[1 - \left[\frac{X_1}{d_{i(i+1)} + X_1 X_2}\right]^3\right]^2 . \tag{2.8}$$

The parameters X_1 and X_2 will be determined by a least-squares fit from empirical data in section 2.4.

Wake Effect and Centerline Deficit Velocity: The wake effect of a leading vehicle yields a reduced air velocity, and hence reduced dynamic pressure, received by a follower vehicle. This velocity deficit can be expressed for a 2-vehicle combination via the maximum deficit velocity rate occuring at the centerline of the wake, *i.e.*,

$$\frac{u_w}{u_s} = 1 - \xi \ . \tag{2.9}$$

The maximum deficit velocity rate in the wake of a vehicle, ξ, is the ratio between the velocity drop at the centerline of the wake and the air velocity received by the vehicle under solo driving. Tadakuma *et al.* provide an analytical expression in [20] for this maximum deficit velocity rate at distance d_{12} between two vehicles at positions 1 and 2 as

$$\xi_1 = \alpha \cdot (C_{Ds,1})^{\beta} \cdot \left(1 - \frac{\Delta C_{Db,1}}{C_{Ds,1}}\right)^{\beta} \cdot \left(\frac{d_{12}}{\sqrt{A_{f,1}}}\right)^{-\frac{2}{3}} \tag{2.10}$$

where, the additional index in the subscripts denotes the corresponding vehicle with 1 leading and 2 following. Then, $C_{Ds,1}$ represents solo driving drag coefficient of the lead vehicle, $\Delta C_{Db,1}/C_{Ds,1}$ is the stagnation pressure correction at the rear base of the lead vehicle, $A_{f,1}$ the projected frontal area, and d_{12} the distance of the follower vehicle. The coefficients α and β have been empirically determined in [20] as $\alpha = 1.05$ and $\beta = 0.2$ for sedan-type passenger vehicles. Note that it is important not to double count effects: although the stagnation pressure is a coupled effect between leader and follower, the drag increasing (negative) effect on

the pushing vehicle is completely absorbed in the maximum velocity rate, while the (positive) impact from being pushed is entirely captivated in the drag coefficient correction. The purpose of this study is the creation of a hybrid prediction model for energy savings in a platoon based upon fitting of a simplified physical model to experimental data. Unfortunately, most studies do not publish drag coefficients or frontal areas of the utilized vehicles employed. One solution could be to estimate the corresponding vehicle parameters in Eq. (2.10) and to only fit α and β to the experimental outcomes. However, we suggest a different approach by decoupling the first two bracketed expressions in Eq. (2.10) and by collecting all vehicle parameters into one unknown variable, yielding

$$\xi_i = X_3 \cdot \left(1 - \frac{\Delta C_{Db,i}}{C_{Ds,i}}\right)^{X_4} \cdot d_{i(i+1)}^{-\frac{2}{3}} \,. \tag{2.11}$$

In order to incorporate Eqs. (2.10) and (2.11) into Eq. (2.6), it should be noted that these velocity drops have been derived for a 2-vehicle combination in which the first vehicle is subject to uniform main flow corresponding to the actual vehicle speed. The ratio $q_{p,i}/q_{s,i}$ in Eq. (2.6), on the other hand, reflects the ratio of the received dynamic pressure by vehicle i in platooning and its dynamic pressure under solo driving. A concatenation of pressure drops would be possible if the ratio of uniform flow equivalent velocities U_{i+1}/U_i were available which include all accumulated effects caused by vehicles in front of the ego vehicle i. Yet, this uniform flow equivalent (corresponding to the actually experienced aerodynamic drag) can precisely be determined from the previously calculated DRRs up to vehicle $i-1$. Hence, the concatenation of the velocity drops yields

$$\begin{aligned} \frac{q_{p,i}}{q_{s,i}} &= \left(\frac{U_2}{u_{s,1}} \cdot \frac{U_3}{U_2} \cdots \frac{U_{i-1}}{U_{i-2}} \cdot \frac{u_{w,i}}{U_{i-1}}\right)^2 \\ &= (1 - DRR_{i-1}) \cdot (1 - \xi_{i-1})^2 \,. \end{aligned} \tag{2.12}$$

As previous considerations have been performed under the assumption of uniform flow, a correction factor accounting for the span-wise parabolic pressure distribution around the centerline of a sedan-type vehicle has been suggested by Tadakuma *et al.* [20]. This correction factor corresponds to an increase of the coefficient of forebody pressure to counteract overestimated wake effects. Yet, the correction value as suggested in [20] is not bounded and exceeds 1 for small inter-vehicle distances. Not only is this a physically inconsistent modification, but it has also been evident that this suggested correction for passenger vehicles is not directly applicable for our approach. However, when concatenating vehicles in a long platoon, a

significant dampening factor must be introduced to keep predictions consistent with real data. This heuristic term is more pronounced for short distances. The observed behavior is potentially due to the considerable differences in aerodynamics between passenger vehicles and heavy-duty trucks with significant unmodeled effects (turbulence) at short distances. As the velocity deficit will be maximum at the center line, the ratio q_p/q_s will overestimate the dynamic drag reduction rate. We achieve excellent results when comparing prediction to actual data from testing with the following concatenation damping for vehicles at position 3 and higher:

$$\Delta C_{Dc,i} = 1 \; + \; \min\left[0.23391, \quad X_5 \cdot e^{X_6 \cdot d_{(i-1)i}}\right]. \tag{2.13}$$

Complete Drag Reduction Model: The unknown ratios q_p/q_s and C_{Dp}/C_{Ds} in Eq. (2.6) can now be expressed via the correction terms modeled above, yielding the following complete model for the drag reduction rate of the ith vehicle in the platoon:

$$\begin{aligned}
DRR_1 &= \frac{\Delta C_{Db,1}}{C_{Ds,1}} \\
DRR_2 &= 1 - \Big\{ (1-\xi_1)^2 \left[1 - \Delta C_{Db,2}/C_{Ds,2}\right] \Big\} \\
DRR_i &= 1 - \Big\{ \left(1 - DRR_{(i-1)}\right) \left(1 - \xi_{(i-1)}\right)^2 \\
&\qquad \times \left(\Delta C_{Dc,i}\right) \left[1 - \Delta C_{Db,i}/C_{Ds,i}\right] \Big\} \\
DRR_N &= 1 - \Big\{ \left(1 - DRR_{(N-1)}\right) \left(1 - \xi_{(N-1)}\right)^2 \left(\Delta C_{Dc,N}\right) \Big\}.
\end{aligned} \tag{2.14}$$

2.4 Prediction Formula Results

The prediction model in Eq. (2.14) has been fitted to the results from the SAE J1321 fuel consumption tests which are summarized in [1]. Here, particularly the data from the 2017 3-Truck and 2-Truck as well as the 2016 3-Truck configurations has been utilized. As existing on-road tests of heavy trucks only report reduction in total fuel consumption, however, data cannot directly be employed for fitting the DRR model. In order to isolate the DRR from total fuel savings, the contribution of the rolling resistance as part of the road load has to be removed, *i.e.*,

$$DRR = FRR \cdot \left[1 + F_R/F_D\right]. \tag{2.15}$$

Here, FRR is the published fuel reduction rate (fuel savings) in [1], F_R corresponds to the load due to rolling resistance, and F_D is the nominal drag force apparent under solo driving. For the nominal drag force, a frontal area of $A_f = 10m^2$ has been determined from the specifications of the truck and trailer combination employed in [1]. No information for the nominal drag coefficient of the utilized truck and trailer combination has been published. Therefore, a low nominal value of $C_D = 0.568$ has been assumed according to [40] as the trailers were outfitted with side-skirts and a boat-tail. The international standard atmosphere at sea level and at 15 degrees Celsius has been applied for the air density, yielding $\rho = 1.225kg/m^3$. For an assessment of the rolling resistance, velocity dependent (dynamic) components have been neglected as their contribution is only a very small fraction compared to the static resistance. A static rolling resistance coefficient of $f_0 = 0.0055$ has been assumed. Whereas the static rolling resistance coefficient is highly tire and surface dependent and varies widely in literature, this particular choice for concrete surfaces has been based upon the average value in a recent study [42]. For the necessary normal forces, the published vehicle mass of $29,400kg$ in [1] has been implemented.

In order to render parameter fitting more robust, the experimental data has been preprocessed by a nonlinear transformation to allow for the application of linear least squares. The stagnation pressure coefficients X_1 and X_2 in Eq. (2.8) have been determined based solely on lead truck data as stagnation pressure is the only apparent effect. For the unknown parameter X_3 and X_4 in Eq. (2.11), the data for the trailing vehicle in 2-vehicle platoons as well as the data for the middle vehicle in 3-vehicle platoons has been utilized. The experimental drag reductions have again been pre-processed by a nonlinear transformation and by removing the stagnation pressure effects via the previously fitted Eq. (2.8). At this point, the residual error between the predicted DRR and the experimental data was examined for the 2^{nd} vehicle. Tadakuma *et al.* [20] suggested to include a nonuniform flow correction for the drag coefficient in Eq. (2.6) for small distances as experimental analysis for sedan-type vehicles exhibited a parabolic shape of the actual velocity distribution. Yet, our fitting approach yielded such a small and unstructured residual error that no further inclusion of their unconstrained nonuniform flow correction has been deemed necessary.

Table 2.1: Summary of Fitting Variables and Parameters

X_1	X_2	X_3	X_4	X_5	X_6
0.1821	1.5216	0.6643	8.9340	0.3371	-0.0419

$m[kg]$	f_0	k	ρ	C_D	$A_f[m^2]$
25370	0.0055	0.00055	1.225	0.686	10

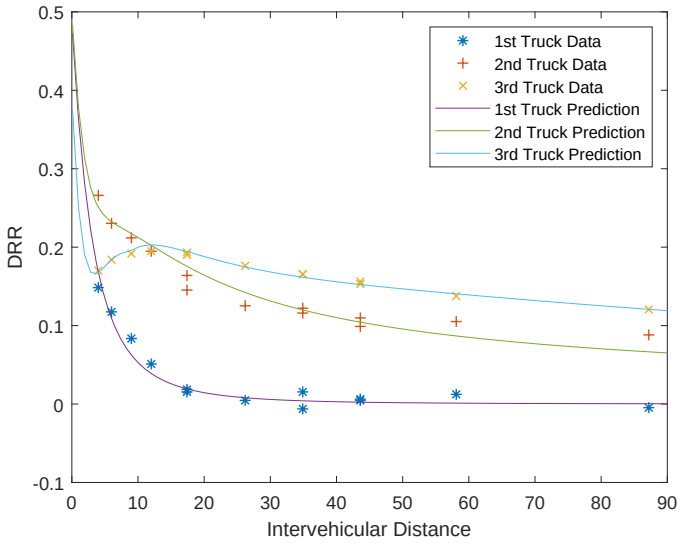

Figure 2.6: DRR Prediction / Experimental Results

A comparison of the predicted results for the last vehicle in 3-vehicle platoons with the experimental data exhibited discrepancies as previously discussed. While this discrepancy was initially thought to be of hyperbolic character in accordance with the physical flow models, a semi-logarithmic plot revealed almost perfect exponential character. With the parameters in Eq. (2.13) fitted to the concatenation error for the 3^{rd} vehicle, the performance of the introduced hybrid prediction model for energy savings in heavy-duty platoons is depicted in Figure 2.6. Here, the developed prediction model exhibits excellent consistency with the actual data for 3-vehicle platoons from [1]. Table 2.1 summarize fitted variables as well as suggestions for all other parameters in Eqs. (2.4) and (2.14). To complete the vehicle specific power model in Eq. (2.4), we suggest to employ an average vehicle mass for simulation in Table 2.1 based upon the average observed mass of class 9 to class 13 vehicles weighted by their actual distribution on road group J as published in [38]. The nominal drag coefficient in Table 2.1 corresponds to the average value for the different tractor-semitrailer configuration as shown in [40].

Chapter 3

Centralized Approach

In this chapter, we mainly present our centralized optimization model, experiments and results. The centralized model is formed as a linear programming model with the aim to make best possible platooning decisions in order to obtain potential maximum energy savings. Plenty of experiments are designed with different parameter combinations. We will present our results grouped according to two criteria: (*i*) Traffic Conditions, (*ii*) Energy Savings. The results related to "Traffic Conditions" will show the number and distribution of vehicles and platoons on the highway. The results related to "Energy Savings" will demonstrate the potential reduction in energy consumption under various traffic conditions.

3.1 Linear Programming Model

Refer to our centralized model, it attempts to find the best vehicle-to-platoon assignments to reduce energy consumption as much as possible. The highway network is divided into platooning zones that are about 1 mile in radius. For each zone the location, speed, and destination of each vehicle and platoon are collected from the simulation model. Then the linear programming model below is solved and output the platooning decisions. Note that, these decisions are considered to maximum estimate energy savings for each platooning zone, which also lead to a maximum for whole system. To ease the exposition of the model, we first introduce the following sets, parameters, and decision variables:

Sets

$\mathbb{P}$: set of all platoons in a given zone ($j \in \mathbb{P}$)
$\mathbb{V}_s$: set of all single vehicles in a given zone ($i \in \mathbb{V}_s$)
$\mathbb{P}_i$: set of all platoons that vehicle i can join
$\mathbb{V}_j$: set of all vehicles in platoon j

Parameters

d_i : current location of vehicle i (including those in a platoon)
n_j : number of vehicles in platoon j
C : maximum number of vehicles allowed in a platoon
M : a large constant (*e.g.*, length of the highway)
w^q : weight assigned to each component of the objective function
S_r : total energy saved (in percentage) by a platoon with r vehicles
D_i : destination of vehicle i
D_k^j : destination of the k^{th} vehicle (sorted by destination) in platoon j
$D_k^{i,j}$: destination of the k^{th} vehicle (sorted by destination) in platoon j if single vehicle i is also part of the platoon

Decision variables

x_{ij} : 1 if vehicle i joins platoon j, 0 otherwise

Given this notation, the optimization model can now be written as

$$\min_{x} \quad \sum_{i\in\mathbb{V}_s}\Bigg\{w^1\Bigg(\sum_{j\in\mathbb{P}_i}\frac{x_{ij}}{n_j}\sum_{k\in\mathbb{V}_j}(|D_i-D_k|-M)\Bigg) \tag{3.1a}$$

$$+w^2\sum_{j\in\mathbb{P}_i}x_{ij}\Bigg(\Big[(D_1^j-d_i)S_{n_j}+\sum_{k=1}^{n_j-2}(D_{k+1}^j-D_k^j)S_{n_j-k}\Big]$$

$$-\Big[(D_1^{i,j}-d_i)S_{n_j+1}+\sum_{k=1}^{n_j-1}(D_{k+1}^{i,j}-D_k^{i,j})S_{n_j-k+1}\Big]\Bigg)\Bigg\}$$

$$\text{s.t.} \quad n_j+\sum_{i\in\mathbb{V}_s}x_{ij}\le C, \qquad \forall j\in\mathbb{P}, \tag{3.1b}$$

$$\sum_{j\in\mathbb{P}_i}x_{ij}\le 1, \qquad \forall i\in\mathbb{V}_s\,. \tag{3.1c}$$

As seen from the mathematical formulation above, the objective function in our optimization model has two terms. The first term is assigned a weight of w^1 and the second a weight of w^2. Because minimizing energy consumption directly would lead to a nonlinear model, which are generally more difficult to solve compared to linear models, we chose to minimize the energy consumption indirectly. To that end, the first term in the objective function is simply creating platoons in which the vehicles have destinations that are close to each other. The intent here is to minimize the number of times vehicles have to join or leave a platoon so that energy is not expended unnecessarily. The second term in the objective function is maximizing the savings of vehicle to platoon assignments. The first half of this term estimates the energy savings for platoon j when vehicle i is not part of the platoon, and the second half estimates the savings with vehicle i as part

of platoon j. Note that since we modeled this as a minimization problem we are considering the negative of the savings. The constraints are relatively straight forward. The first constraint (3.1b) simply says that the current number of vehicles in a platoon plus all the new vehicles that are assigned to join this platoon should not exceed the capacity which is set to 5 ($C = 5$). The second constraint (3.1c) ensures that each single vehicle is assigned to at most one platoon. The S_r values used in the objective function are compiled from the experimental results mentioned in our literature review and shown in Table 3.1.

Table 3.1: Estimated energy savings based on position in the platoon*

	Number of vehicles in the platoon			
Position	**2**	**3**	**4**	**5**
1	3%	3%	3%	3%
2	10%	12%	12%	12%
3		13%	14%	14%
4			14%	15%
5				15%
	$S_2 = 13\%$	$S_3 = 28\%$	$S_4 = 43\%$	$S_5 = 59\%$

* values reflect an estimate of accumulated savings for the entire platoon with respect to a single vehicle's consumption as a base value

3.2 Experiments and Parameters

To evaluate our centralized linear model, we conducted 16 experiments and a limited sensitivity analysis. In each experiment, the simulation model begins with an empty system and runs for 4 hours ($T = 4\ hrs$). The results are recorded and computed with both a 4 hour period and a last two hour period because it takes about two hours for the system to reach steady-state. Only results for the last two hours are reported considering the number of experiments are large. Single vehicles enter the highway from each of the on-ramps at a flow rate of 150 (or 100) vehicles per hour (vph) for different experiments. The first number in column three of Table 3.2 shows the input flow rate for each experiment. The second number in column three lists the rate with which platoons enter the highway. When this number is 180 (120), it indicates that a platoon enters the highway section in Lane 2 at mile zero 20 (30) seconds after a platoon has entered in Lane 3 at mile zero. In other words, 180 (120) platoons enter the highway each hour (half from Lane 2 and the other half from Lane 3). Each experiment is initialized with the same random seed to ensure a fair comparison and analysis, and a total of exactly 24,095 (16,034) vehicles go through the system in each simulation run based on the input rates in column three of Table 3.2. The fourth column shows the desired speed of the platoons in Lane 2. Notice that, the platoons in Lane 3 travel at a desired speed of $65mph$ for all experiments.

Table 3.2: Summary of Experimental Parameters

Experiment	w^{1*}	Vehicle†/Platoon‡ Input	Speed* (mph)	Optimization
1	0.25	150 / 180	55	On
2	0.25	150 / 180	60	On
3	0.25	100 / 120	55	On
4	0.25	100 / 120	60	On
5	0.125	150 / 180	55	On
6	0.125	150 / 180	60	On
7	0.125	100 / 120	55	On
8	0.125	100 / 120	60	On
9	0	150 / 180	55	On
10	0	150 / 180	60	On
11	0	100 / 120	55	On
12	0	100 / 120	60	On
13	NA	150 / 180	55	Off
14	NA	150 / 180	60	Off
15	NA	100 / 120	55	Off
16	NA	100 / 120	60	Off

* coefficient of the first term in objective function (3.1a)

† vehicles per hour from each on-ramp, ‡ platoons per hour from mile zero

* desired speed of platoons in Lane 2

As seen in the last column of Table 3.2, in experiments 1-12 the optimization model is active indicating that single vehicles on the highway are allowed to join platoons. In experiments 13-16 the optimization model is turned off, *i.e.*, single vehicles are not allowed to join platoons. Note, however, that there are still platoons in experiments 13-16, but these are platoons that enter from mile zero and are not newly formed. The optimization model is run every 20 seconds ($\tau = 20s$) in experiments 1-12 and provide essential information to optimization. Recall that our optimization model has two terms in its objective function with weights w^1 and w^2 (with $w^1 + w^2 = 1$), where w^1 weights the first term in our objective function assigning vehicles to platoons based on their destinations. The second term, with weight w^2, distributes vehicles to platoons based on estimated savings. The second column in Table 3.2 lists the different weights w^1 (with $w^1 + w^2 = 1$) employed in our optimization.

As shown in Figure 2.1 and summarized 2.1, the simulation and optimization models interact continuously in experiments 1-12. Throughout this iterative process, data is collected every $0.5s$. Specifically, we record the vehicle ID, current speed, acceleration, location, headway, platoon ID, and position in platoon for each vehicle every 0.5 simulation seconds resulting in large amounts of data. To ease the analysis of the data collected, we developed a Matlab routine that generates figures and tables some of which are presented in Sections 3.3 and 3.4. Part of this post-analysis includes the energy savings calculations which utilize the prediction models detailed in Section 2.3.

3.3 Traffic Results

In this section, we primarily concentrate on reporting 4 different distributions referring to distribution of vehicles, distribution of vehicles by platoon size, distribution of platoons by size, and distribution of vehicle by position in platoon.

Table 3.3 lists the average distribution of the vehicles over the last two simulation hours, *i.e.*, in steady-state. For example, for the last two hours of Experiment 1, vehicles traveled in a platoon on average 41% of the time and were single vehicles for the remainder of time. As expected, vehicles spent the least amount of time in a platoon in Experiments 13-16 as the optimization model is not active in these runs and, thus, new platoon formations are not allowed.

Table 3.3: Distribution of Vehicles in the System*

Experiment	Single Vehicles	Vehicles in Platoons
1	59%	41%
2	61%	39%
3	64%	36%
4	66%	34%
5	58%	42%
6	61%	39%
7	64%	36%
8	65%	35%
9	55%	45%
10	57%	43%
11	61%	39%
12	64%	36%
13	90%	10%
14	91%	9%
15	90%	10%
16	91%	9%

* in steady-state, *i.e.*, average over the last two hours

We also observe a difference in the average amount of time spent in a platoon in Experiments 1-4 vs. 5-8 vs. 9-12. In Experiments 9-12, where $w^1 = 0$, vehicles spent more time in platoons (*e.g.*, on average 45% for Experiment 9). This suggests that the first term in the objective function of our optimization model is not contributing to the formation of more platoons. Recall that the first term forms platoons based on vehicle destinations. Thus, increasing w^1 creates platoons that stay together for longer periods of time, but this comes at the expense of forming fewer platoons overall. As will be discussed later, lower values of w^1 also seem to lead to more energy savings. Hence, it is reasonable to assign more weight to the second term in our optimization model, *i.e.*, yielding high w^2 and low w^1. The full results, including averages and standard deviations of the number of vehicles on the highway (in addition to the percentage distribution), are provided

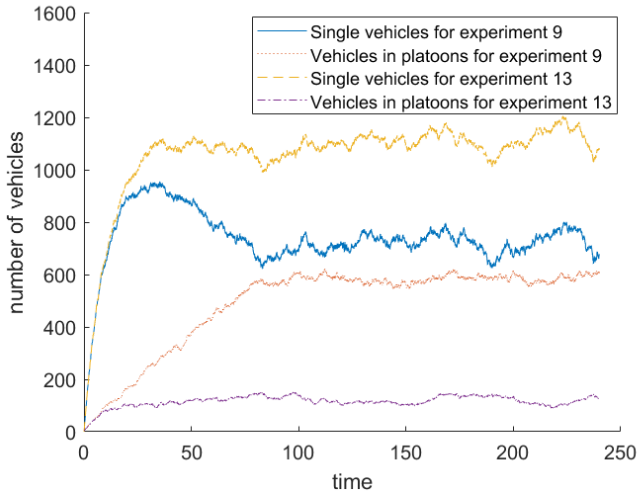

Figure 3.1: Number of vehicles and platoons for Experiments 9 and 13

in the Appendix A in Table 10.

Whereas Table 3.3 provides the average distribution over the last two hours for all experiments, Figure 3.1 depicts the exact number of vehicles for Experiments 9 and 13 over the full four hours. The top (yellow, dashed) graph shows the number of single vehicles in Experiment 13 varying between 1000 and 1200. The line below it (solid blue) illustrates the number of single vehicles in Experiment 9. Then, the orange, dotted graph right below depicts the number of vehicles in platoons in Experiment 9. Finally, the purple line at the bottom shows the number of vehicles in platoons in Experiment 13. Note that the average values reported in Table 10 match what is observed in Figure 3.1. In Experiment 13, we reach steady-state after approximately 40 minutes, but in Experiment 9 it takes about 80 minutes to arrive at steady-state. For those experiments with platooning decisions, platoons take around 80 to 90 minutes from mile zero to close to the end of the highway if they are not disbanded. Thus, these experiments need more time to reach steady-state. Nevertheless, we consistently consider the first two hours as our warm-up period for all experiments, as mentioned earlier. We choose to focus on Experiment 9 in more detail as it resulted in the highest percentage of vehicles traveling in platoons. Since Experiment 13 corresponds to the same settings of Experiment 9 but without the optimization, the comparisons provide valuable insights. For example, Experiments 1 and 5 utilize the same settings as 9, but with differing values for w^1. Examining the percentage of vehicles in platoons in Experiments 13, 1, 5, and 9 (in that order), we can notice a significant increase with 10% to 41% to 42% to 45%, respectively.

Table 3.4 details the distribution of vehicles by platoon size. Clearly, the percentage of vehicles

in platoons of size 5 is the smallest in Experiments 13-16 as new platoon formations are not allowed. In Experiments 9-12, we observe not only more vehicles in platoons (see Table 3.3), but also an increased number of them in platoons of size 5 (see Table 3.4). In Experiment 9, for instance, approximately 45% of all vehicles are in a platoon at any point in time, and of those in a platoon about 49% are in one with 5 vehicles.

Table 3.4: Distribution of Vehicles by Platoon Size*

Experiment	Size			
	5	**4**	**3**	**2**
1	46%	30%	17%	7%
2	46%	30%	17%	7%
3	43%	30%	19%	8%
4	40%	31%	21%	8%
5	48%	30%	16%	6%
6	45%	30%	17%	8%
7	44%	30%	18%	8%
8	41%	30%	21%	8%
9	49%	30%	15%	6%
10	47%	30%	16%	7%
11	45%	30%	18%	7%
12	42%	30%	20%	8%
13	15%	21%	29%	35%
14	15%	21%	29%	35%
15	15%	19%	26%	40%
16	15%	19%	26%	40%

* in steady-state, *i.e.*, average over the last two hours

Figure 3.2 illustrates the breakdown of platoons (not vehicles in platoons) by size for Experiments 9 (left) and 13 (right). In Experiment 9, most of the platoons are of size 5 followed by platoons with 4 vehicles then 3- and 2-vehicle platoons. As expected, larger platoons are encouraged in our centralized model on account of more energy savings. Notice that there is a limited number platoons of size 1 appearing for short periods of time as shown at the bottom of the figure. If a single vehicle, for instance, is in the process of joining a 3-vehicle platoon and two of the vehicles leave this platoon before the joining operation is completed, then the Vissim output records this as a 1-vehicle platoon. This occurs less than 1% of the time. Thus, we do not report the 1-vehicle platoons in Tables 3.4, 3.5, 11, and 12. In contrast to Experiment 9, we see that most of the platoons are of size 2 followed by 3-, 4-, and 5-vehicle platoons in Experiment 13. It also makes sense since no other vehicles join platoons, but vehicles leave when reaching destinations.

Similar to what we observe in Figure 3.1, we can see in Figure 3.2 that it takes longer to reach steady-state in Experiment 9 compared to 13. In any case, the system is stable during the last two hours for all experiments. Whereas Figure 3.2 depicts the exact number of platoons by size over the full four hours, Table 3.5 provides the average distribution for all 16 experiments over the last two hours. Once again, in Experiments 13-16 the number of 2-vehicle platoons (around 50 %) is higher than any other platoon size

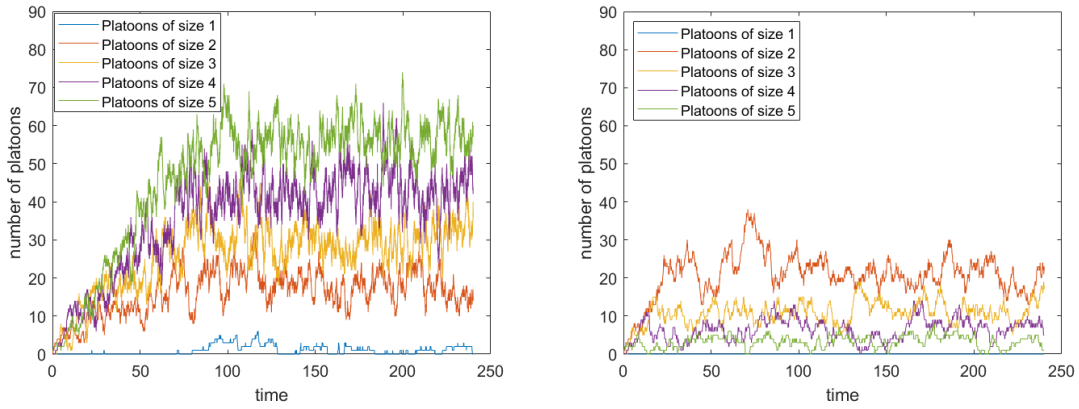

Figure 3.2: Number of platoons by size for Experiments 9 (left) and 13 (right)

whereas in Experiment 9 we observe more 5-vehicle platoons (39 %).

Table 3.5: Distribution of Platoons by Size*

Experiment	Size			
	5	**4**	**3**	**2**
1	36%	29%	22%	13%
2	35%	28%	22%	15%
3	33%	28%	24%	15%
4	30%	28%	26%	16%
5	37%	30%	21%	12%
6	34%	28%	21%	17%
7	34%	29%	23%	14%
8	31%	28%	26%	15%
9	39%	29%	20%	12%
10	36%	29%	22%	13%
11	35%	28%	23%	14%
12	32%	28%	25%	15%
13	8%	15%	28%	49%
14	8%	15%	28%	49%
15	9%	13%	24%	54%
16	9%	13%	24%	54%

* in steady-state, *i.e.*, average over the last two hours

We also assessed statistics on the number and percentage of vehicles by their position in a platoon as given in Tables 3.6 and 13. Comparing Experiments 1-12 with 13-16, we see a clear difference in the total time vehicles spend in specific positions in platoons (again due to the optimization being turned off in Experiments 13-16). Among Experiments 1 to 12, we did not observe significant differences, thus indicating that different parameters we tested did not impact the average time a vehicle spends in a specific position. Pay attention to positions 1 and 2, since platoons own a minimum size which is 2, the percentage of position 1 and 2 should equal. However, as we mentioned before, a little bit platoons temporarily have size 1. Thus, percentage of position 1 can be equal or slightly larger than percentage of position 2. In particular, the

percentage of time spent in position 5 in Experiment 9 results as 10% being slightly higher than the rest of the experiments. Also, more other figures are shown in Appendix B.

Table 3.6: Distribution of Vehicles by Position in Platoon*

Experiment	Position				
	1	**2**	**3**	**4**	**5**
1	26%	26%	22%	17%	9%
2	26%	26%	22%	17%	9%
3	26%	26%	23%	16%	9%
4	27%	27%	22%	16%	8%
5	26%	26%	22%	17%	9%
6	27%	26%	22%	16%	9%
7	26%	26%	23%	16%	9%
8	27%	27%	22%	16%	8%
9	26%	25%	22%	17%	10%
10	26%	26%	22%	17%	9%
11	26%	26%	23%	16%	9%
12	27%	27%	22%	16%	8%
13	35%	35%	18%	9%	3%
14	35%	35%	18%	9%	3%
15	36%	36%	17%	8%	3%
16	36%	36%	17%	8%	3%

* in steady-state, *i.e.*, average over the last two hours

Before we continue to discuss our results related to energy savings, we would like to point out some specific traffic conditions we observed in our simulations.

1. Some vehicles assigned to join platoons reach their destinations before the joining process with their corresponding target platoons is completed. In this case, these vehicles cancel their joining processes and prepare to leave the system.

2. During the time in which some vehicles attempt to join a target platoon, all but one vehicle in this target platoon leave. This platoon does not disband and waits for others to join. This is the reason why there exists platoons with only one vehicle.

3. Since there is a difference in desired speed between lane 2 and lane 3, some single vehicles affect platoons by blocking platoons with lower speed. Additionally, some platoons driving in different lanes can cause localized congestion. Under these circumstances, single vehicles will take longer to cover a distance to complete the joining procedure. This situation is similar to the scenario when heavy trucks cause localized delay on a freeway where other vehicles are queued up behind it.

4. Since acceleration is randomly distributed (assigned by Vissim), some vehicles may accelerate very slowly in catching up with other vehicles ahead in platoons when a gap appears. Due to these slow

accelerations, the gap distances may increase before the following vehicle's speed exceeds the leading vehicle's, at which point the gap distances will gradually reduce.

3.4 Energy Consumption Results

As mentioned in Section 2.3, three distinct and important energy consumption phenomena account for the main difference between vehicles traveling singly or in a platoon. These are acceleration, rolling friction, and aerodynamic drag reduction. The drag reduction ration (DRR) as determined in Section 2.3 is a ratio based upon the original drag coefficient for solo driving C_D for each vehicle. Thus, we consider typical low (0.568), average (0.686), and high (0.863) values for C_D when assessing energy consumption.

Table 3.7: Energy Savings over the Last Two Hours

Experiment	Total Energy			Acceleration	Time in
	Low C_D	Avg C_D	High C_D	Energy	Platoon*
1 vs. 13	1.01%	2.18%	3.52%	-48.99%	41 vs. 10%
5 vs. 13	1.28%	2.47%	3.84%	-48.99%	42 vs. 10%
9 vs. 13	1.40%	2.68%	4.15%	-52.56%	45 vs. 10%
2 vs. 14	-0.10%	0.98%	2.22%	-49.09%	39 vs. 9%
6 vs. 14	-0.92%	0.35%	1.81%	-60.80%	39 vs. 9%
10 vs. 14	0.43%	1.60%	2.94%	-51.74%	43 vs. 9%
3 vs. 15	1.57%	2.46%	3.48%	-39.64%	36 vs. 10%
7 vs. 15	1.62%	2.54%	3.58%	-40.64%	36 vs. 10%
11 vs. 15	1.58%	2.63%	3.81%	-47.20%	39 vs. 10%
4 vs. 16	1.29%	1.96%	2.72%	-29.94%	34 vs. 9%
8 vs. 16	1.52%	2.18%	2.93%	-28.56%	35 vs. 9%
12 vs. 16	1.61%	2.31%	3.11%	-30.72%	36 vs. 9%
9 vs. 10	1.17%	1.33%	1.53%	-1.65%	45 vs. 43%
11 vs. 12	0.08%	0.48%	0.94%	-15.08%	39 vs. 36%

* average percent time a vehicle spent in a platoon in steady-state

Table 3.7 summarizes the energy savings results. Note that Experiments 1, 5, and 9 are compared to 13 since they employ the same problem parameters. Here, the only differences are in the objective function coefficients w^1 and w^2. Likewise, Experiment 14 is compared to 2, 6, and 10, Experiment 15 to 3, 7, 11, and Experiment 16 to 4, 8, and 12. Columns 2, 3, and 4 in Table 3.7 show the savings realized as a result of optimized platoon assigning, respectively for low, average, and high values of C_D. The largest savings are

observed in Experiment 9 with a high C_D, as expected. Recall that Experiment 9 is the one in which vehicles spent a higher percentage of their time in platoons and a higher percentage of the platoons were 5-vehicles platoons. Naturally, a high drag coefficient yields higher absolute savings when platooning. Specifically, in Experiment 9 vehicles spent on average 4.15% less energy compared to Experiment 13. While this may not seem a large improvement at first sight, it is important to note that in Experiment 9 vehicles spent 52.56% more energy to maintain vehicles in formation through acceleration losses. Even with this increased effort, the system as a whole still yields energy savings when our proposed optimization model is activated. Moreover, experiments with larger w^2 values seem to consume a bit more energy from acceleration due to more forming process. However, Experiment 6 is an exception. The primary reason for Experiment 6 consuming more energy in acceleration is that some locally congestion happens as well as more blocking situations occur in order that more acceleration engages in. In addition to that, if we compare Experiment 9 with 10, and Experiment 11 with 12, Experiments 9 and 11 result less total energy consumed and more energy consumed by acceleration. Nevertheless, we cannot conclude that such experiments have better energy savings because they are not compare with the same experiment with optimization turned off. For example, experiment 12 saves more energy than 11 in low C_D. The exact energy consumption values are detailed in the Appendix A in Tables 14 and 15. The savings reported in Table 3.7 correspond to the energy consumed during the last two hours as reported in Table 14.

Chapter 4

Decentralized Approach

Unlike the centralized control method, when individual vehicles enter the freeway, they prefer to picking the most valuable choice for themselves to save energy. Thus, their aims are not to obtain the most potential savings for some platoons or entire road traffic, however, they focus on optimizing their own savings. Therefore, a decentralized agent-based model will be introduced in this Chapter. With similar organization as Chapter 3 for centralized model, besides the decentralized formulation, experiments and two types of results (*i*) Traffic Conditions results, (*ii*) Energy Savings results are presented here as well.

4.1 Dynamic Game Formulation

In this decentralized formulation, these individual vehicles and platoons are not related. Then, they cannot share their information such as destinations. They only know those information can be observed when they enter the main freeway. Based on this precondition, we would like to consider each individual vehicle as a player of this decentralized model. These players are actual competitors in order to obtain self best profits.

Such being the case, we formulate our decentralized model as a dynamic game. In this game, assume each player is rational, and only seeks its maximum potential profit. As we defined in Section 2.2, single vehicles (players) are only allowed to join platoon behind. Hence, when an individual (player) decides to join a platoon, it will become the lead vehicle of the new platoon. In addition, we assume that players notice some locally observed information such as the number of vehicles in available platoons, the desired speed of platoons for different lanes, the number of players, and order of players to take action, which depends on relative location of these individual vehicles (players). We also assume that players are not able to predict

future profit. Thus, rewards of players in this game only depend on best current result, which contain two parts: primarily, potential energy savings, and, secondarily, time to destinations. If and only if there is a tie in primary part of rewards, secondary part of rewards will be compared for decision. Similarly, simulation-optimization framework is utilized here, and simulation and energy settings remain same too.

According to these settings, we then introduce our dynamic game model with complete information.

Indices

i : Player (Individual vehicle) index

j : Action (Platoon) index

Sets

$\mathbb{V}_s$: set of all players (single vehicles) in a given zone ($i \in \mathbb{V}_s$)

$\mathbb{P}_i$: set of all actions (platoons) that player (vehicle) i can take (join) when they move including the action, which is stay as an individual vehicle ($j \in \mathbb{P}_i$)

Parameters

O_i : moving sequence of player (vehicle) i

n_j^i : number of vehicles in platoon j include those players (individual vehicles) took (decided to join) actions (platoons) j before i

C : maximum number of vehicles allowed in a platoon

p_l^j : energy saved (in percentage) in position l by taking action j (platoon), where j (platoon) has a size $r = 2,3,4,5$ after all players take actions

t_j : time to reach destinations by taking action j (platoon) (there is only two choices: fast and slow)

Decision variables

a_i : action of player (individual) i takes

Players: All individual vehicles in each platooning zone ($\mathbb{V}_s$) are the players of the dynamic game in that zone.

Sequence of move: According to relative current locations for all players in one platooning zone, the player who has the closest distance to available platoons will firstly take action. Then, the player with second closest distance will take action next and so on. In other words, players take actions in order from back to front since available platoons are always behind.

Actions of players when they move: When player moves, all available platoons ($\mathbb{P}_i$) are optional actions for that player. Note that, this set of available platoons may change with previous players taking actions so that some platoons reach their capacity. In addition to this, not to join any of available platoons is also an action. If player takes this action to stay as a single vehicle, then, $a_i = 0$.

Payoffs: $v_i(.)_{i \in \mathbb{V}_s}$ represents the payoff of player i. Based on preceding players' actions, when player i moves, player i will know current size of available platoons, and current lanes those platoons on. If

available platoons on Lane 3, time to destination will be represented as fast because desired platoon speed is larger on that lane. Otherwise, if available platoons on the Lane 2, time to destination will be marked as slow. If player i takes an action to join an available platoon, player i will also notice its position in that target platoon. Then, the payoff of player i can be written as $v_i(a_1, a_2, ..., a_n) = (p_l^j, t_j)$. For instance, if player 4 becomes the third vehicle of a platoon with 5 vehicles in Lane 3 after all players finishing their moving, the payoff of player 4 will be $v_4(a_1, a_2, ..., a_n) = (14\%, fast)$ according to Table 4.1. The p_l^j values are compiled from the experimental results shown in Table 4.1.

Table 4.1: Estimated energy savings based on position in the platoon*

	Number of vehicles in the platoon			
Position	**2**	**3**	**4**	**5**
1	3%	3%	3%	3%
2	10%	12%	12%	12%
3		13%	14%	14%
4			14%	15%
5				15%

* values reflect an estimate of savings with respect to a single vehicle's consumption as a base value

According to current consideration, if there exists at least one available slot in any of optional platoon, player always chooses one action to join a platoon instead of staying alone.

Proof: Since we do not consider energy consumed or wasted during the process to enter a platoon in our payoffs, for potential platooning energy savings according to Table 4.1, the minimum payoff of energy saving percentage is 3%, which is greater than 0 (no saving). As we mentioned before, only if there is a tie exists in primary part of payoff, secondary part, time to destination, will affect the decision. Therefore, no matter those remaining platoons with a fast speed or not, rational player will select one action to join a platoon for better payoff. In other words, as long as there exists available slot, the action, stay individual, is dominated by other actions. Hence, to simplify our model, we won't consider stay individual as a positive action. This action will only exist when there is no other options.

Game tree: The extensive-form of this game is diagrammatic described as a game tree in Figure 4.1. In this game tree, each layer records one player's information. Nodes in each layer represents the player's different statuses just before its move. For example, the layer 0, which only includes root, represents the situation of the first player in sequence just before its move. All nodes are named based on their layers. For example, $x_{ln-1,1}$ can be explained as the first nodes in layer $n-1$. Branches under root or each leaf node, represent all actions that moving player can take at that time. For instance, those branches under root represent different actions that the first player can take. This tree, from top layer to bottom, shows the sequence from

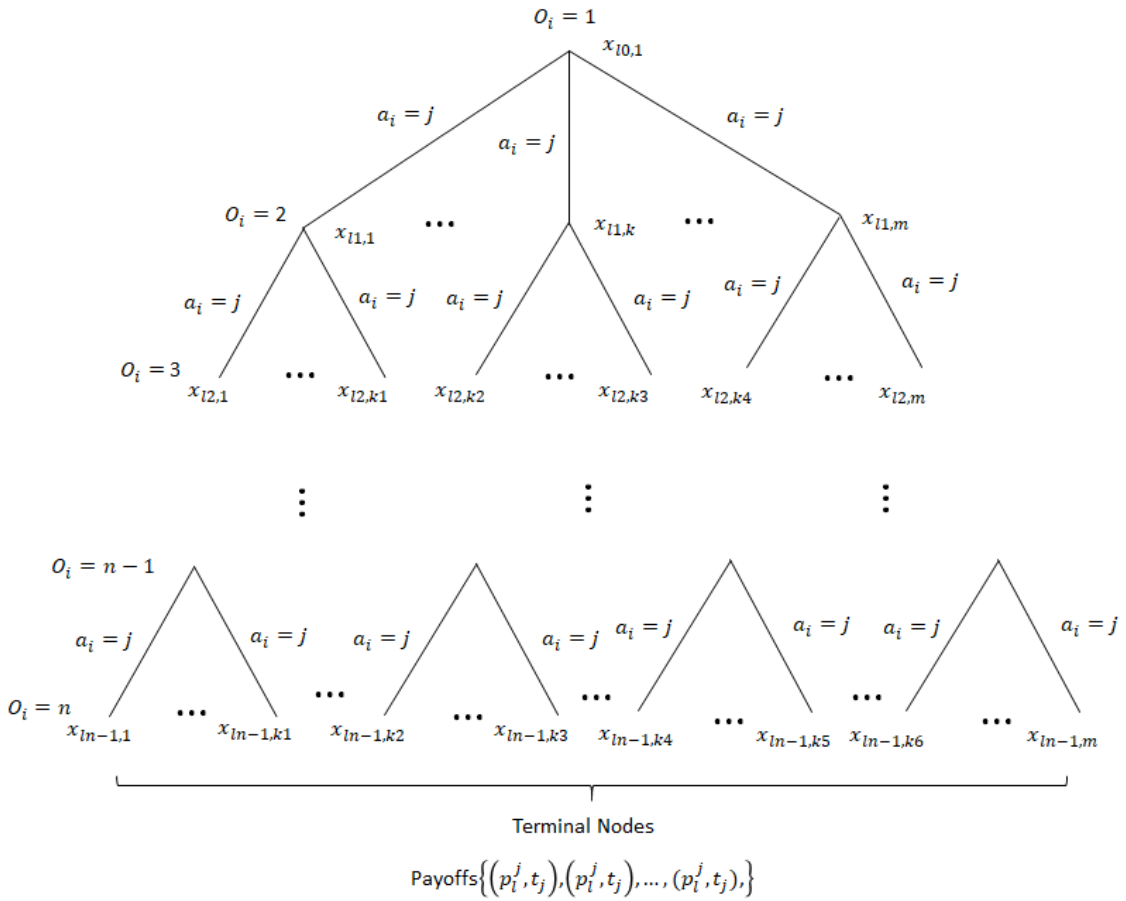

Figure 4.1: Game Tree of Dynamic Game

first player to last player. All nodes, after the last player's actions, are terminal nodes. For each of these terminal nodes, payoff of each player will be recorded based on the path from root to this node.

Method and Nash equilibrium: As we mentioned before, all players should be rational at every stage of the game. More specifically, players use strategies that are the best responses to their opponents' strategies at every information set in our game tree. This principle is called sequential rationality [43]. According to Tadelis [43], a proposition and a corollary are introduced below:

Proposition 1. *Any finite game of perfect information has a backward induction solution that is sequentially rational, Furthermore if no two terminal nodes prescribe the same payoffs to any player then the backward induction solution is unique.*

Corollary 1. *Any finite game of perfect information has at least one sequentially rational Nash equilibrium in pure strategies. Furthermore if no two terminal nodes prescribe the same payoffs to any player then the*

game has a unique sequentially rational Nash equilibrium.

Refer to our dynamic game, our game is a finite game with perfect information since there are finite number of individual vehicles in every platooning zone, and every player knows exactly where it is in the game based on what happened before. Therefore, as shown in the proposition and corollary, backward induction is a method to retrieve sequentially rational Nash equilibrium in pure strategies.

In addition to this, we introduce the definition of subgame-perfect Nash equilibrium in Tadelis [43]. A strategy profile is a subgame-perfect Nash equilibrium if it represents a Nash equilibrium for every proper subgame of the extensive-form (original) game. Note that, every subgame-perfect Nash equilibrium is a Nash equilibrium, but not all Nash equilibria are necessarily subgame-perfect equilibrra. For finite game of perfect information, a fact from Tadelis [43] explained below:

Fact 1. *For any finite game of perfect information, the set of subgame-perfect Nash equilibria coincides with the set of Nash equilibria that survive backward induction.*

Hence, backward induction is used to solve our dynamic game with perfect complete information. Nevertheless, the complexity of utilizing backward induction is not good. Considering our game tree of extensive form, time complexity to solve this game using depth-first implementation is $O(b^h)$, and space complexity to store this tree is $O(bh)$. Notice that, b is the branching factor, while h is the height of the tree. More precisely, b represents the number of platoons available (actions), and h represents the number of single vehicles (players) in each platooning zone. Although the time complexity is exponential, in each platooning zone, there are not too many platoons since platoons are generated every 20 (30) seconds. On the other hand, vehicle input rate for each ramp is not large so that there are not too many single vehicles as well.

4.2 Experiments and Parameters

To evaluate our decentralized model using our simulation-optimization framework, 4 pairs of experiments are set up. Each pair of experiments include one experiment with dynamic game model, and one without. All experiments begin with empty network and run for a 4 hour period ($T = 4\ hrs$). Table 4.2 shows the summary of experimental parameters.

The second column shows the vehicle and platoon input flow rate per hour. The single vehicle input flow rate (vph) 150 (or 100), which is the first number in column two, represents there is an average of 150 (or 100) single vehicles enter this freeway through each on-ramp per hour. As we mentioned in Section 2.2,

Table 4.2: Summary of Experimental Parameters for Dynamic Game Model

Experiment	Vehicle†/Platoon‡ Input	Speed⋆ (*mph*)	Game
1	150 / 180	55	On
2	150 / 180	60	On
3	100 / 120	55	On
4	100 / 120	60	On
5	150 / 180	55	Off
6	150 / 180	60	Off
7	100 / 120	55	Off
8	100 / 120	60	Off

† vehicles per hour from each on-ramp, ‡ platoons per hour from mile zero

⋆ desired speed of platoons in Lane 2

platoons are generated in both Lane 2 and Lane 3. Hence, the second number in the second column, 180 (or 120) shows the number of platoons entering from the beginning of the freeway (half from Lane 2 and the other half from Lane 3). In other words, 180 (or 120) indicates that a platoon enters the highway section in Lane 2 at mile zero 20 (30) seconds after a platoon has entered in Lane 3 at mile zero. Same with settings in Section 3.2, to ensure a fair comparison, each experiment is initialed with same random seed. According to different input flow rates, a total of exactly 24,095 (16,034) vehicles go through the system in each simulation run.

The third column indicates the desired speed of platoons while driving in Lane 2. Note that the desired speed of platoons in Lane 3 is always set up to 65*mph* for all experiments.

Experiments (1,5), (2,6), (3,7), (4,8) are 4 pairs with and without our optimization game model. Note that, for experiments 5 to 8, although the optimization is turned off, there are still platoons in the simulation, but these platoons are entering from mile zero.

4.3 Traffic Results

Traffic condition result will show the number and distribution of vehicles and platoons on the freeway. As we discussed before, simulation starts with an empty network. Thus, there exists a warm up period, in which traffic flows reach steady-state gradually. Similar to Section 3.3, we mainly report results of steady-state during the last two hours. In Table 4.3, average distribution of vehicles is reported over the last two hours (in steady-state). For instance, average 43% of vehicles travelled in a platoon at a time step, for the last two hours of Experiment 1. The rest is for individual vehicles. In the way that was expected, Experiments 1-4 show that more number of vehicles travel in a platoon comparing Experiments 5-8 due to the game model

is not active, in other words, individual vehicles are not able to join platoons. In addition, Experiments 1-2 provide more platooning opportunities for single vehicles than Experiments 3-4, thus, higher percentages of vehicles appear in platoons in Experiments 1-2.

Table 4.3: Distribution of Vehicles in the System*

Experiment	Single Vehicles	Vehicles in Platoons
1	57%	43%
2	57%	43%
3	62%	38%
4	65%	35%
5	90%	10%
6	91%	9%
7	90%	10%
8	91%	9%

* in steady-state, *i.e.*, average over the last two hours

On the other side, Figure 4.2 and Figure 4.3 depicts the exact number of vehicles for Experiments pair (1,5) and (3,7) over the full four hours. From the left graphs of both figures, it is clear that steady-state will be reached after 80 minutes for Experiments 1 and 3. Otherwise, it takes 40 minutes for Experiments 5 and 7 to reach steady-state. Therefore, we consistently consider the first two hours as our warm-up period for all experiments. After steady-state reached, the lines representing number of single vehicles and vehicles in platoons become stationary. The top (blue, solid) lines show the number of individual vehicles, while the bottom (red, dashed) lines show the number of vehicles travelling in a platoon. Figures 4.2 and 4.3 have similar shapes, but different numbers of vehicles sole or in platoons. In particular, there is a larger gap between single vehicles and vehicles in platoons in Experiment 3 by contrast to Experiment 1. In other word, the average percentages reported in Table 4.3 match what is observed in Figures 4.2 and 4.3.

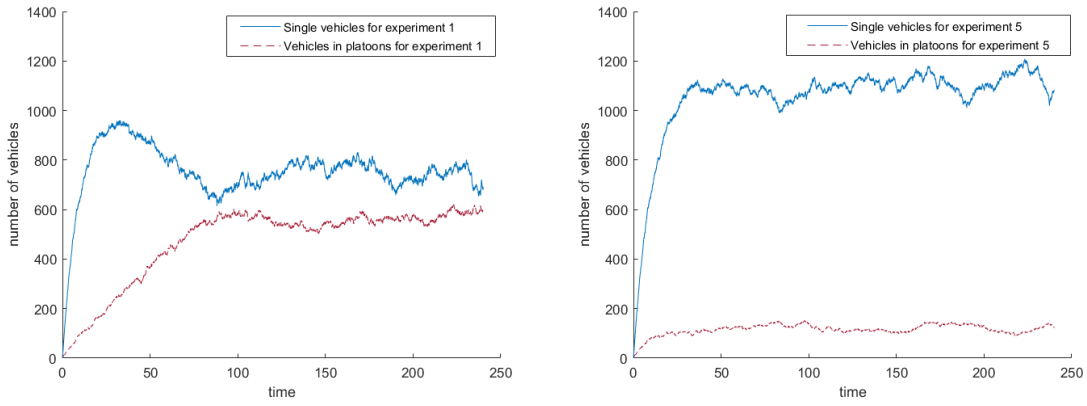

Figure 4.2: Number of vehicles and platoons for Experiments 1 (left) and 5 (right)

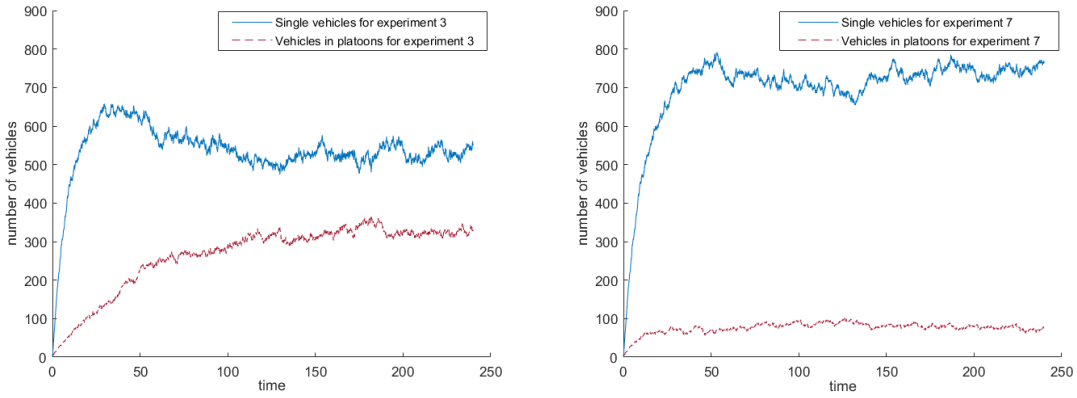

Figure 4.3: Number of vehicles and platoons for Experiments 3 (left) and 7 (right)

Table 4.4 provides details on distribution of vehicles by positions in platoons. For all experiments, it is distinct that the percentage of front vehicles in platoons is larger than the percentage of back vehicles except the comparison between the first and the second position. The reason is that the number of vehicles in platoons within a range from 2 to 5. In other words, all platoons with a lead vehicle, first position, and may not have latter positions (*e.g.*, a platoon with size 3 has position 1 to 3, but not 4 and 5). Moreover, there is some but not many platoons with only one vehicle in the system on account of the reason some individual vehicles under process to join these platoons. Therefore, the percentage of position 1 is equal to or slight larger than position 2. Comparing Experiments 1-4 with 5-8, we see a obvious difference for the proportion of vehicles in specific positions in platoons (due to the game model being turned off in Experiments 5-8). Among Experiments 1-4, there is not a significant difference, thereby indicating that different parameters we tested did not impact the proportion of vehicles in a specific position.

Table 4.4: Distribution of Vehicles by Position in Platoon*

Experiment	**Position**				
	1	**2**	**3**	**4**	**5**
1	27%	26%	22%	16%	9%
2	27%	26%	22%	16%	9%
3	27%	27%	22%	16%	8%
4	27%	27%	23%	15%	8%
5	35%	35%	18%	9%	3%
6	35%	35%	18%	9%	3%
7	36%	36%	17%	8%	3%
8	36%	36%	17%	8%	3%

* in steady-state, *i.e.*, average over the last two hours

One of the most important factors to illustrate traffic conditions is the platoons with different sizes. Tables 4.5 and 4.6 state the distribution of vehicles by platoon size and distribution of platoons by size,

respectively. From Table 4.5, explicitly, there is an increase as the size of platoon becoming larger in Experiments 1-4. Oppositely, a decrease exists in Experiments 5-8. For Experiments 5-8, since new platoons are not permit to form, existing platoons, which are generated from beginning, will eventually disband after vehicles leave one by one. In Experiments 1-4, not only more vehicles are in platoons (see Table 4.3), but also an increased number of them in platoons of size 5 (see Table 4.5). For example, approximately 43% of all vehicles are in a platoon at any point in time, and of those in a platoon about 43% are in one with 5 vehicles for Experiment 1. Note that, although there are more vehicles in platoons with larger size based on Table 4.5, we may not observe more platoons with larger size. According to Table 4.6, for Experiments 1-4, percentages of number of platoons with size 5 are slightly larger than platoons with size 4.

Table 4.5: Distribution of Vehicles by Platoon Size*

Experiment	**Size**			
	5	**4**	**3**	**2**
1	43%	31%	18%	8%
2	43%	31%	18%	8%
3	40%	32%	20%	8%
4	38%	31%	22%	9%
5	15%	21%	29%	35%
6	15%	21%	29%	35%
7	15%	19%	26%	40%
8	15%	19%	26%	40%

* in steady-state, *i.e.*, average over the last two hours

Table 4.6: Distribution of Platoons by Size*

Experiment	**Size**			
	5	**4**	**3**	**2**
1	33%	29%	23%	15%
2	33%	30%	23%	14%
3	30%	29%	25%	16%
4	28%	28%	27%	17%
5	8%	15%	28%	49%
6	8%	15%	28%	49%
7	9%	13%	24%	54%
8	9%	13%	24%	54%

* in steady-state, *i.e.*, average over the last two hours

Figures 4.4 and 4.5 illustrate the breakdown of platoons by size for Experiments pair (1,5) and (3,7), respectively. For both figures, green line, purple line, yellow line, orange line, and blue line represent platoons with size 5,4,3,2, and 1. As we mentioned before, there is a limited number of platoons of size 1 (blue line) appearing for short periods of time as shown at the bottom of the graph. Recall that, if a single vehicle, for instance, is in the process of joining a 2-vehicle platoon and one vehicle leaves this platoon before the joining process is completed, then the Vissim output records this as a 1-vehicle platoon. The average percentage of

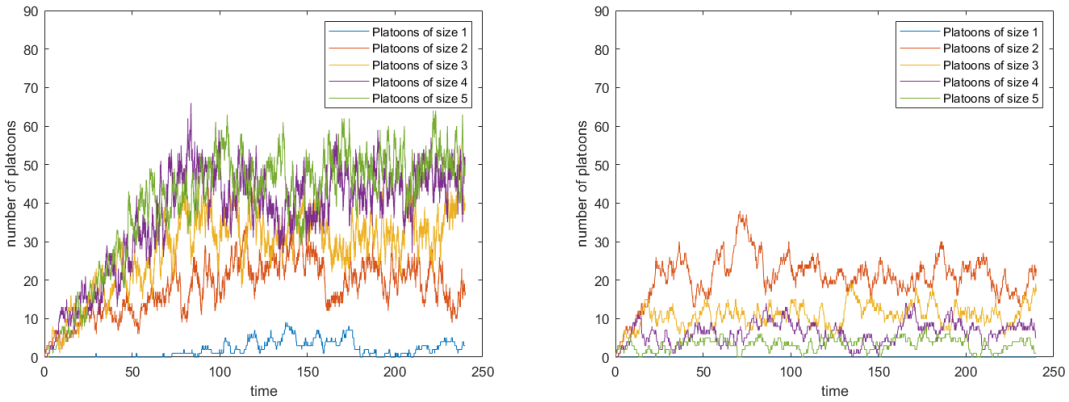

Figure 4.4: Number of platoons by size for Experiments 1 (left) and 5 (right)

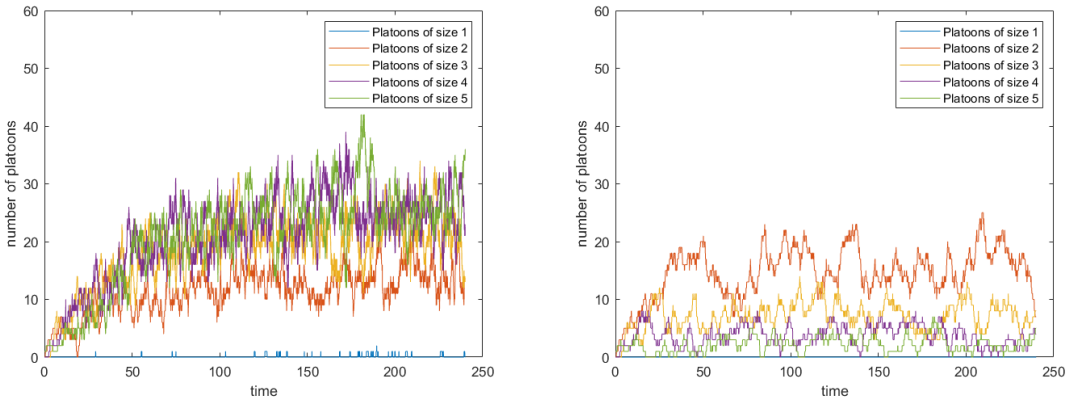

Figure 4.5: Number of platoons by size for Experiments 3 (left) and 7 (right)

platoons with size 1 is usually less than 2% in these experiments. Thus, we ignore reporting the 1-vehicle platoons in Tables 4.5, 4.6. Comparing two blue lines in Figures 4.4 and 4.5, the number of platoons with size 1 in Experiment 1 is larger than in Experiment 3 primarily based on larger traffic flow and locally congestion. For platoons with other sizes in Experiments 1 and 3, most of the platoons contain 5 and 4 vehicles (*i.e.* green line and purple line are intertwined), followed by 3- and 2- vehicle platoons. It is clear that 5-vehicle platoons in Experiment 1 is slight more than 4-vehicle platoons. However, this situation is not very clear in Experiment 3. Table 4.6 also proves this feature. On the contrary, in Experiments 5 and 7, we observe that most of the platoons are of size 2 followed by 3-, 4-, and 5-vehicle platoons, and no 1-vehicle platoon.

We can observe that in both Figures 4.4 and 4.5 that it takes more time to reach steady-state in experiments with platoons forming compared to experiments without. Similar to Figures 4.2 and 4.3, it takes around 80 minutes for experiments with optimization, and around 40 minutes for without. In any case, the

system is stable during the last two hours for all experiments. In terms of Table 4.6, it records distribution of platoons for all experiments, while Figures 4.4 and 4.5 depicts the exact number of platoons over the entire simulation period. Other figures are provided in Appendix B.

4.4 Energy Consumption Results

Energy savings result will demonstrate the potential reduction in energy consumption under various traffic conditions. In Section 2.3, we develop a prediction energy model based on the formula in Tadakuma *et al.* [20]. Recall that three distinct and crucial energy consumption phenomena, which are aerodynamic drag reduction, acceleration, and rolling friction, account for the primary difference between vehicles traveling individually or in a platoon. As we shown in Section 2.3, we define the drag reduction rate (DRR) as a ratio on account of the original drag coefficient for solo driving C_D for each vehicle. For this part of results, three types of values,low (0.568), average (0.686), and high (0.863), for C_D are considered to calculate energy consumption. Differing from the way we report energy consumption results in centralized formulation, since there are not too many experiments, energy consumption results are analyzed in detail for both entire four hour time period and last two hour (steady-state) period.

Table 4.7: Energy Savings of Experiment Pair (1,5)

Experiment 1 and 5	**Total Energy**			**Acceleration Energy**	**Percentage in Platoon**	
	Low C_D	Average C_D	High C_D		**Mileage**	**Time**
1 (last two hours)	351,023	388,616	445,004	70,960	41%	43%
1 (entire four hours)	661,651	734,390	843,500	124,244	37%	39%
5 (last two hours)	349,417	392,632	457,453	42,276	9%	10%
5 (entire four hours)	662,594	744,433	867,192	80,809	9%	10%
1 vs. 5 (last two hours)	-0.46%	1.02%	2.72%	-67.85%	454%	440%
1 vs. 5 (entire four hours)	0.14%	1.35%	2.73%	-53.75%	399%	390%

Table 4.8: Energy Savings of Experiment Pair (2,6)

Experiment 2 and 6	**Total Energy**			**Acceleration Energy**	**Percentage in Platoon**	
	Low C_D	Average C_D	High C_D		**Mileage**	**Time**
2 (last two hours)	350,698	389,337	447,297	65,633	43%	43%
2 (entire four hours)	662,021	736,541	848,321	115,876	38%	39%
6 (last two hours)	350,101	393,556	458,738	41,807	9%	9%
6 (entire four hours)	664,097	746,416	869,895	79,951	9%	10%
2 vs. 6 (last two hours)	-0.17%	1.07%	2.49%	-56.99%	476%	468%
2 vs. 6 (entire four hours)	0.31%	1.32%	2.48%	-44.93%	414%	409%

Although our decentralized decisions are determined by dynamic game among individual vehicles, where each single vehicle pays attention to its own payoff, we want to evaluate whether entire system is benefit from these individual decisions. Tables 4.7, 4.8, 4.9, and 4.10 summarize energy consumption and savings results for each pair of experiments. Note that, Experiments (1,5), (2,6), (3,7), (4,8) are four pairs including an experiment which allows to form platoon and the other prohibits with same parameters. Tables 4.7, 4.8, 4.9, and 4.10 contain three major parts, which are energy consumption of first experiment (*i.e.* row 2 and 3), energy consumption of second experiment (*i.e.* row 4 and 5), energy savings by contrast with two experiments (*i.e.* row 6 and 7). For every part, we report both results over the last two hours (*i.e.* in steady-state) and over entire four hours. Columns 2, 3, and 4 in Tables 4.7, 4.8, 4.9, and 4.10 provide the energy consumption in kilowatt hour (kWh) of the whole system, respectively for low, average, and high values of C_D. In addition, column 5 shows the energy consumption from acceleration perspective. Pay attention to the first and the second part of these tables, energy consumed over four hours is always less than twice energy consumed over the last two hours on account of warm-up process. During the warm-up period, vehicle and platoon amount is less than usual since network starts with empty traffic. Third part of these tables record the percentage of energy savings comparing to experiments with and without platoon forming. According to column 2, 3, and 4 in these tables, energy consumption reduced from -0.46% to 3.40% for the whole system,

Table 4.9: Energy Savings of Experiment Pair (3,7)

Experiment 3 and 7	**Total Energy**			**Acceleration Energy**	**Percentage in Platoon**	
	Low C_D	Average C_D	High C_D		**Mileage**	**Time**
3 (last two hours)	223,639	249,260	287,691	35,038	36%	38%
3 (entire four hours)	428,482	478,446	553,393	63,538	31%	33%
7 (last two hours)	226,578	255,078	297,828	24,107	9%	10%
7 (entire four hours)	433,574	488,145	570,001	46,184	9%	10%
3 vs. 7 (last two hours)	1.30%	2.28%	3.40%	-45.35%	393%	386%
3 vs. 7 (entire four hours)	1.17%	1.99%	2.91%	-37.57%	342%	337%

Table 4.10: Energy Savings of Experiment Pair (4,8)

Experiment 4 and 8	**Total Energy**			**Acceleration Energy**	**Percentage in Platoon**	
	Low C_D	Average C_D	High C_D		**Mileage**	**Time**
4 (last two hours)	224,028	250,615	290,494	30,772	34%	35%
4 (entire four hours)	429,590	481,044	558,225	57,312	30%	31%
8 (last two hours)	226,817	255,476	298,464	23,588	9%	9%
8 (entire four hours)	434,117	489,007	571,341	45,166	9%	9%
4 vs. 8 (last two hours)	1.23%	1.90%	2.67%	-30.46%	372%	369%
4 vs. 8 (entire four hours)	1.04%	1.63%	2.30%	-26.89%	329%	327%

where negative percentage represents more energy consumed instead of savings. Based on column 5, energy savings from acceleration within a range from -67.85% to -26.89%. In other words, experiments with platoon forming always consume more energy in acceleration prospective. Tables 4.7 and 4.8 summarize results for experiments with same platoons and vehicles input rate. Thus, these experiments all have 24095 vehicles in total. As shown in Tables 4.7 and 4.8, total energy consumed in experiments with faster speed in Lane 2 is a bit more than with slower speed. Oppositely, energy consumed from acceleration is smaller. Tables 4.9 and 4.10 have similar results. This mainly depends on locally congestion according to slow speed in Lane 2. Referring to total energy savings, Table 4.7 offers a range (-0.46%,2.73%), while Table 4.8 provides a range (-0.17%,2.49%). For the reason we did not make decisions based on system level, more entering and leaving processes happen causing more energy waste from acceleration. Therefore, for low value of C_D, platooning gives rise to a little bit energy waste with 0.46% and 0.17%. Energy savings in consideration of high value of C_D are fairly good. Unlike previous experiments, Tables 4.9 and 4.10 show results of experiments with 16034 vehicles. Percentages of total energy savings for these experiments offer better performance of platooning with ranges (1.17%,3.40%) and (1.04%,2.67%). Comparing 4.7 and 4.8 with 4.9 and 4.10, it is obviously that percentages of energy loss from acceleration are much different. For example, energy consumed from acceleration for Experiment 1 is 67.85% more than it for Experiment 5. On the other hand, energy consumed from acceleration for Experiment 3 is 45.35% more than it for Experiment 7. Moreover, column 6 and 7 record the percentage of mileage and time travelled in platoons, respectively for different experiments. The percentage of time perfectly matches those values in Table 4.3. The percentage of mileage travelled in platoons usually equal or a little bit less than the percentage of time. Additionally, around 4.5 (3.8) times platoons are in Experiments 1 and 2 (3 and 4) by contrast with Experiment 5 and 6 (7 and 8). Based on these results, we indeed observe energy savings through platooning, even though decisions are made decentralized and concentrate on personal profits.

Chapter 5

Energy Consumption of One Single Platoon

Our simulation traffic network contains a lot of platoons and single vehicles. In order to understand energy consumed by platoons in-depth, instead of analyzing global consumption, we would like to pay attention to observing an individual platoon in this chapter. Different factors, which potentially are able to impact energy consumed by a platoon, are applied to experiments desired in this chapter so as to evaluate performance of the particular platoon. Results are then provided for analysis.

5.1 Problem Description and Experiments Desired

In our simulation-optimization framework, through our prediction energy consumption model, we are able to calculate precise energy consumption in system-wide. In other word, total energy consumed by all vehicles during entire time period are reported. As we know, this energy consumption illustrates performance of all single vehicles and platoons under real traffic conditions. However, we cannot know how much a platoon contributes in term of total energy consumption. In particular, we won't know the detail of energy consumption in those three main factors, aerodynamic drag, acceleration, and rolling fraction, mentioned in Section 2.3. In addition, we would like to observe the energy consumption based on vehicle position in a platoon.

There are several factors could potential affect platoons, not only in energy consumption, but also

in traffic capacity and safety. In our paper, we mainly focus on energy aspect. As we described in Chapter 1, inter-vehicle distance and speed can potentially impact air drag reduction as well as acceleration. Additionally, platoons with larger size can yield to more energy savings on account of accumulated air drag reduction effect. Thus, we would like to observe that individual platoon according to these three factors.

We design these experiments utilizing our simulation-optimization framework as a background traffic situation. Refer to simulation model, we apply parameters from Experiment 12 in Section 3.2, including vehicle and platoon input rate as 100 and 120, and desired speed 60mph on Lane 2. On the other hand, new platoons forming are on with centralized approach containing weight $w^1 = 0$. Based on these settings, we record traffic background information in simulation model at the end of hour 2 as initialization for experiments of individual platoon. To do so, we can initialize these experiments in steady-state rather than starting with a warm-up period. In other word, we only need to run experiments for two hours in steady-state so as to reduce simulation time. With these presetting, we generate a single platoon for observing at time 10 second to avoid collision with current entering platoon. This individual platoon enters from mile zero on Lane 3, and travels to the end of highway. Thus, it needs to drive 100 miles to reach their destinations. Note that, all vehicles in this platoon have destinations at the end of highway, and no vehicle will leave the platoon until they reach their destinations. Then, no other vehicle can join this platoon as well. Information of vehicles in this platoon is recorded every 0.5 seconds for further analysis.

Table 5.1: Summary of Experimental Parameters for an individual platoon

Experiment	**Factor***	**Headway** (s)	**Speed** (mph)	**Platoon Size**
1	Base	0.7	60	4
2	Headway	0.5	60	4
3	Headway	0.6	60	4
4	Headway	0.8	60	4
5	Headway	0.9	60	4
6	Headway	1.0	60	4
7	Speed	0.7	55	4
8	Speed	0.7	57.5	4
9	Speed	0.7	62.5	4
10	Speed	0.7	65	4
11	Platoon Size	0.7	60	2
12	Platoon Size	0.7	60	3
13	Platoon Size	0.7	60	5
14	Platoon Size	0.7	60	6
15	Platoon Size	0.7	60	7

* factors that different from base setting

In term of three factors mentioned above, we design 15 experiments shown in Table 5.1 with different parameters settings. There is a base experiment setting. By contrast, every other experiment contains only one parameter which is different from base value. Column 2 provides the factor that is different from base setting,

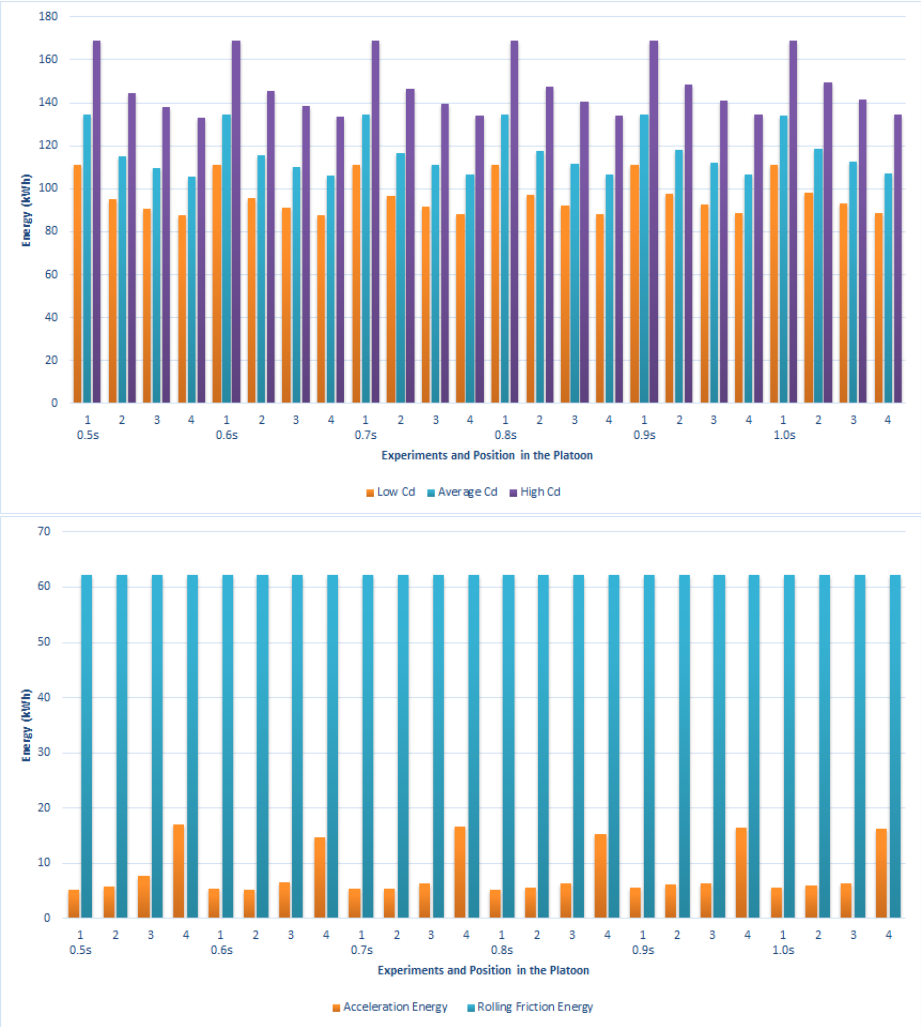

Figure 5.1: Energy consumption from aerodynamic drag (top) and acceleration and rolling friction (bottom) for different Headway

while column 3,4, and 5 show parameters of headway, speed, and platoon size respectively. For example, Experiment 10 includes a different speed 65mph other than base value 60mph, but other parameters are same. Notice that, we use headway with unit second instead of actual inter-vehicle distance here. Additionally, since speed of the platoon is vary, in order not to block platoons behind, desired speed of platoons on Lane 3 are set to the same speed of this single platoon.

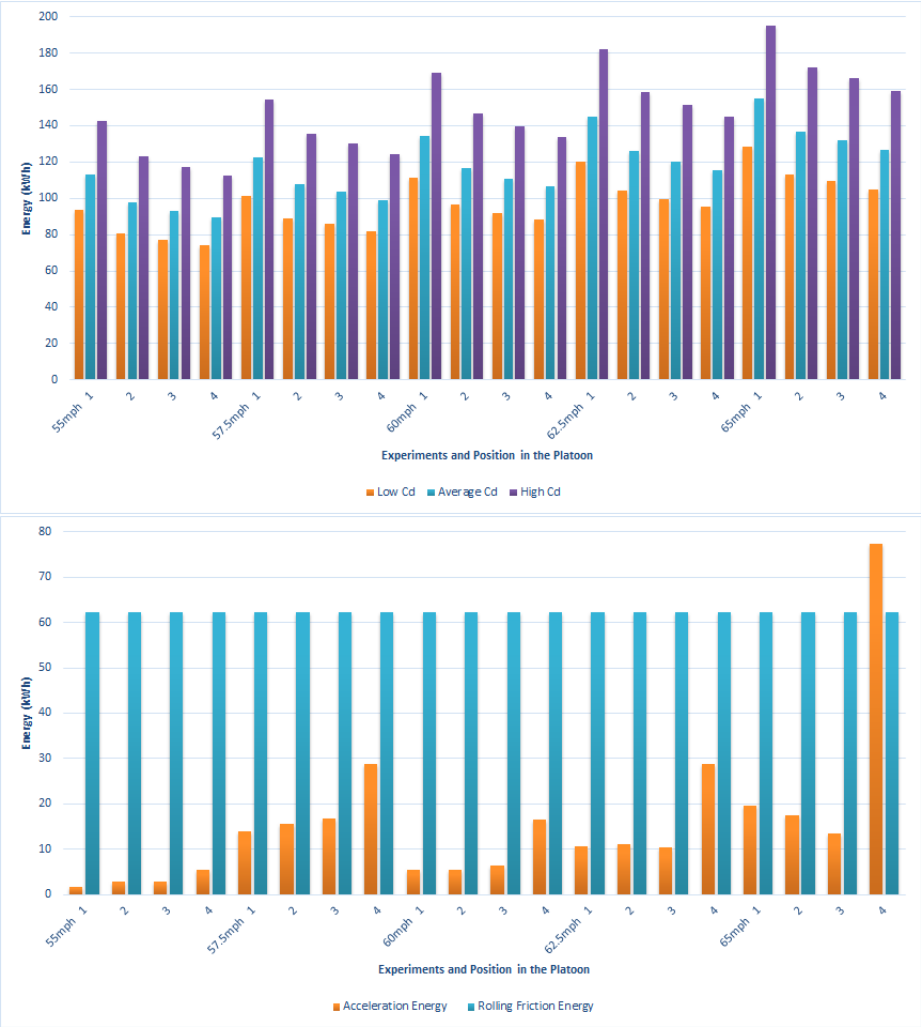

Figure 5.2: Energy consumption from aerodynamic drag (top) and acceleration and rolling friction (bottom) for different Speed

5.2 Results and Analysis

In this section, using the data collected from simulation, MATLAB scripts are applied to compute energy consumed for each vehicle in that individual platoon. Recall that, in Section 2.3, three major factors impact energy consumption. Therefore, we separate total energy into three parts, which are energy from aerodynamic drag, acceleration, and rolling friction. Moreover, we group our experiment results into three sections in order to compare the influence of different values for the same factor. Experiments 1 to 6 are in a group for headway, and Experiments 1, and 7 to 10 are in section for speed, finally, Experiments 1, and 11 to 15 are in group for platoon size.

Figure 5.1 illustrates energy consumption for different headway, where top graph provides energy from air drag with low, average, and high coefficient, and the bottom graph shows the energy from acceleration and rolling friction. In the top graph, orange, blue, and purple bar represent low, average and high drag coefficient. As expected, for each experiment and each vehicle in the single platoon, high drag coefficient lead to the largest energy consumption, followed by average, and low. In addition, considering every experiment, position 1 consumes the largest energy, followed by 2, 3, and 4. It perfectly matches what is shown in Figure 2.6, since inter-vehicle distance for 60mph with 0.5 seconds headway is around 15 meters. In addition, inter-vehicle distances become larger when we enlarge headway. Hence, it indeed follows this decreasing trend. Additionally, there is no much difference for same position in this single platoon among these experiments. This also makes sense on account of gentle descent in Figure 2.6. There is some distinction in values shown in Table 16 in Appendix A. On the other hand, orange bar in the bottom graph illustrates energy from acceleration, while blue bar represents for rolling friction. According to these orange bars, for each experiment, front vehicles consume less energy from acceleration comparing with back vehicles. Particularly, the last vehicle consumed obviously more energy in acceleration prospective. This may depend on more adjustments made for the last vehicle to maintain proper headway. Comparing different experiments, energy from acceleration for same position in this single platoon are similar. Refer to energy from rolling friction, all blue bars shown here are almost same. Thus, rolling friction is not affected by position in platoons as well as inter-vehicle distance.

In terms of speed, results are offered in Figure 5.2. Same with Figure 5.1, top graph has same format for energy from air drag, and bottom graph has same format for energy from acceleration and rolling friction. Based on the top graph here, comparing different positions in the single platoon for every experiment, we can obtain a similar result as shown in Figure 5.1, which is front position consumed more in energy from air drag. Nevertheless, by contrast with different experiments, it is clear that experiments with larger speed consume more energy in all (low, average, and high) drag coefficients. Note that, this is not the energy savings for each vehicle in the individual platoon. It is true that faster speed leads to larger energy consumption. Switching to the bottom graph, energy from rolling friction represented as blue bars are still almost same. It means rolling friction is not impacted by speed as well. However, considering energy from acceleration, the patter that front vehicles consume less than back still exists except experiment with speed 65mph. In addition, experiment with speed 57.5mph seems to consume more energy than experiments with faster speed (*i.e.* 60mph and 62.5mph). Remember that we simulate our network in real traffic situation, these abnormal statuses can be caused by some blocking issues in front of the platoon. Due to this reason, more accelerating and decelerating

Figure 5.3: Energy consumption from aerodynamic drag (top) and acceleration and rolling friction (bottom) for different Size

behaviors are conducted so that vehicles consume more energy from acceleration.

One other important factor here is platoon size. As shown in Table 3.1, platoons with large size potentially make more energy savings. We would like to see what happens based on this factor. Figure 5.3 illustrates energy consumption of the individual platoon by different sizes. Similarly, top graph is for aerodynamic drag, and bottom is for acceleration and rolling friction. For each experiment, back vehicles yield to less energy consumption, in other words, more energy savings from air drag are obtained for back vehicles. When we look at different experiments, vehicle in same position has approximate energy consumption from air drag. Thus, with the decreasing trend, it is obvious that larger size of platoons can save more energy. In consideration of the bottom graph, same status exists for rolling friction. However, there is some variation in

energy from acceleration. It looks like that back vehicles consume more energy in acceleration prospective, but not always. For example, experiment with platoon size 7, fourth vehicle consumes more energy from acceleration than fifth and sixth vehicles. It is reasonable since acceleration is a factor that can be easily influenced by traffic.

Based on these results, we can conclude that energy consumption according to aerodynamic drag follows our prediction energy model as well as results in literature. In addition, energy consumption from rolling friction is stable and is not impacted by these factors. Moreover, energy consumed from acceleration can be affected in some cases, and it provides negative efforts for energy savings. To get better energy savings by platooning, an effective method is to reduce energy consumption from acceleration. Additional complete tables with values are reported in Appendix A.

Chapter 6

Comparisons and Conclusions

In this chapter, a comparison is conducted between centralized and decentralized models. Both criteria, traffic situation and energy consumption, are used to analyze and evaluate the difference. In this comparison, system-wide energy savings are the primary evaluation criteria. After that, the conclusion and future work will be presented in this chapter.

6.1 Comparison between Centralized and Decentralized Models

In this section, we will evaluate the performance of our decentralized formation by comparing with our former centralized model. As described in Chapter 3, centralized model encourages vehicles to form platoons with best possible system-wide savings. Moreover, there is a factor encourage single vehicles to from more stable platoons too. While discussed in Chapter 4, decentralized model aims to maximize potential personal payoffs based on local information observed by individual vehicles. In particularly, platoons formed by this method may not offer best savings in system-wide. We would like to find out the differences between centralized and decentralized models. Throughout our experiments in centralized model, we observed that a weight (w^1) with value zero leads to maximum energy savings. In this case, single vehicles prefer to join platoons rather than remain individual. Therefore, similar to our decentralized setting, single vehicles try to maximize their own savings so that they usually join platoons if possible. Hence, Experiments 1 to 4 in Table 4.2 and Experiments 9 to 12 in Table 3.2 are selected for comparison. Note that, in following comparison, we refer Experiments 9 to 12 in centralized model as Experiments 1 to 4.

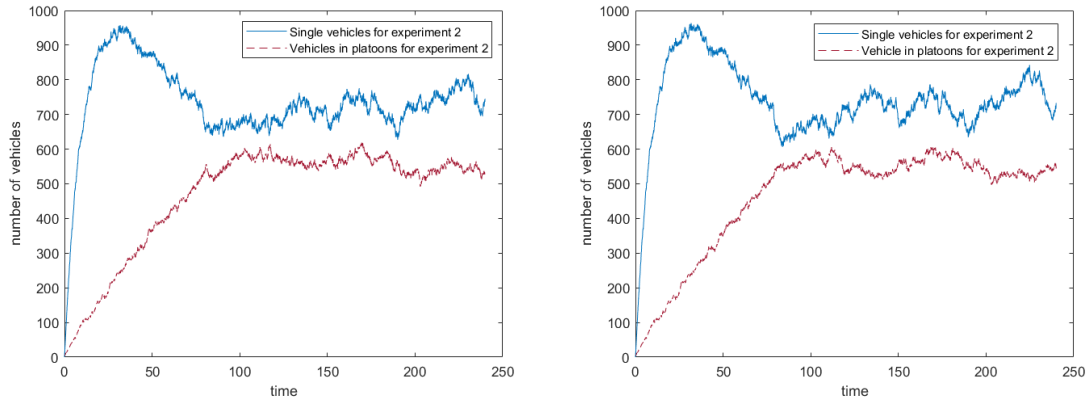

Figure 6.1: Number of vehicles and platoons for Experiment 2 with Decentralized (left) and Centralized (right) model

6.1.1 Traffic condition comparison

In order to analyze the difference in traffic situation, we report distribution of vehicles in Table 6.1. In Table 6.1, first column identifies experiments index. Meanwhile, second column and third column present the percentage of single vehicles and vehicles in platoon respectively. Every two rows, starting with the second row, provide information for both decentralized and centralized distribution. According to these percentages, decentralized model has similar traffic composition to centralized model. For instance, Experiment 2 has an average 57% of vehicles driving individually, and 43% of vehicles in platoons for both decentralized and centralized results. This situation can be observed in Figure 6.1 too, that is, the shapes of both lines in the graph of decentralized model (left) are similar to those in centralized model (right). It makes sense since the optimization part of both models always encourage individual vehicles to join platoons. Note that, as we mentioned above, we only consider the weight (w^1) with a value of zero here for our centralized model.

Table 6.1: Distribution of Vehicles for decentralized and centralized results*

Experiment	Single Vehicles	Vehicles in Platoons
1(Decentralized)	57%	43%
1(Centralized)	55%	45%
2(Decentralized)	57%	43%
2(Centralized)	57%	43%
3(Decentralized)	62%	38%
3(Centralized)	61%	39%
4(Decentralized)	65%	35%
4(Centralized)	64%	36%

* in steady-state, *i.e.*, average over the last two hours

Such being the case, we wonder whether both formulations have the same mean. Therefore, we conduct a T-test to analyze the difference. Since in steady-state, traffic flow is more stable. In other words, number of vehicles driving singly or in platoons will not change sharply. Accordingly, we partition last two hours (120 minutes) to thirty 4 minutes intervals, and average vehicle amount in platoons of this 4 minutes period are calculated as statistical individuals. Thus, a sample is established with 30 individuals for an experiment. Additionally, parameter settings and random seeds remain same for each experiment. That is, traffic situation should be the same when we eliminate the effect of optimization. As shown before, the distribution of vehicles in platoons for both centralized and decentralized model are approximate equal. Then, we make null hypothesis as both models with the same population mean, and alternative hypothesis as their population means are unequal. In our T-test, we present centralized sample as first sample (*i.e.* with μ_1), and decentralized sample as second (*i.e.* with μ_2). The population variance of two models are unknown, but with our calculation, the ratio of sample standard deviations between two models within a range $0.5 < S_{X_1}/S_{X_2} < 2$. As a result, both models have similar population variances. Table 6.2 provide the results of T-test for Experiments 1 to 4. In this table, the first row declare the hypothesis defined, and column 2 and 3 show the confidence interval (CI) we selected and α values. Additionally, column 4 and 5 calculate the t values and p values, while column 6 and 7 provide judgements for results. Refer to confidence interval, we pick 95 %, then α is 0.05. Based on these information in Table 6.2, it is very clear that we reject the null hypothesis with large t value computed for Experiments 1 and 3 since the critical value for t distribution is $\pm$ 2.002. The difference between centralized and decentralized models is highly significant, confirmed by p values. Conversely, null hypothesis cannot be rejected in Experiments 2 and 4. Notice that, t values for these experiments are close to critical values, meanwhile, p values offer a marginally significant difference as well. Therefore, we cannot conclude number of vehicles in platoons for both models have same population mean even though they are observed similar. In particular, t value for Experiment 2 is negative, while others are positive. This provides a sign that sometime decentralized model may possibly include potential more number of vehicles in platoons than centralized model.

In addition to comparing number of single vehicles and vehicles in platoons, platoon amount by different sizes is also an important factor for comparing two models. Table 6.3 provides the distribution of platoons by size for both model. Columns 2 to 5 represent the average percentages of platoons with different sizes. Each experiment also has a pair of data reported for decentralized on top, and centralized on bottom. Based on these information, it is clear that number of 5-vehicle platoons in centralized model account for a larger proportion by contrast with decentralized one. In view of 4-vehicle platoons, both decentralized and

Table 6.2: T-test for number of vehicles in platoons*

Hypothesis: $H_0 : \mu_1 = \mu_2, H_1 : \mu_1 \neq \mu_2$						
Experiment	Confidence Interval (CI)	α	t	p value	Conclusion	Significance
1	95%	0.05	5.038	0.000	reject H_0	highly significant
2	95%	0.05	-1.782	0.080	fail to reject H_0	marginally significant
3	95%	0.05	3.077	0.003	reject H_0	highly significant
4	95%	0.05	1.975	0.053	fail to reject H_0	marginally significant

* in steady-state, *i.e.*, average over the last two hours

centralized formulations have almost same proportion. Moreover, decentralized model owns relatively higher percentages for 3-, and 2- vehicle platoons. Giving an example such as Experiment 2, centralized model has 3% higher for 5-vehicle platoons than decentralized one. On the other side, 1% less for other sizes platoons. Figure 6.2 shows number of platoons by size for both decentralized model in Experiment 2, illustrating on the left graph, and centralized model on the right graph. It is obviously that more 5-vehicle platoons than 4-vehicle platoons in centralized model. On the contrary, the line representing 5-vehicle platoons interweaves with the line for 4-vehicle platoons in decentralized model. If we compare both graphs, lines representing 2-, 3-, and 4- vehicles in the left graph are a little bit higher than in the right graph. Note that, both graphs have the same scale.

Table 6.3: Distribution of Platoons by Size for Decentralized and Centralized results*

Experiment	**Size**			
	5	**4**	**3**	**2**
1(Decentralized)	33%	29%	23%	15%
1(Centralized)	39%	29%	20%	12%
2(Decentralized)	33%	30%	23%	14%
2(Centralized)	36%	29%	22%	13%
3(Decentralized)	30%	29%	25%	16%
3(Centralized)	35%	28%	23%	14%
4(Decentralized)	28%	28%	27%	17%
4(Centralized)	32%	28%	24%	16%

* in steady-state, *i.e.*, average over the last two hours

In this case, T-tests are proceeded to show whether they are different in mean for 5-, and 4- vehicle platoons. Since more platoons with larger size potentially yield to larger energy savings, we only test platoons with 4 and 5 vehicles. So as to design T-test for 5-, and 4- vehicle platoons, as we observed in Table

6.3, 5-vehicle platoons should be compared whether population mean in centralized model is larger. Besides, 4-vehicle platoons can be assumed with same population mean. Therefore, with similar setting mentioned before, we partition last two hours as thirty 4 minutes intervals, and create samples for centralized and decentralized models. Thus, null hypothesis of these T-tests are that both models have same population mean, but alternative hypothesis for 5-vehicle T-test is to assume centralized model has larger mean (*i.e.* one side T-test), while different means for 4-vehicle T-test. Similarly, α is 0.05 (*i.e.* 0.025 for one side), and both comparing samples have similar sample standard deviations (*i.e.* $0.5 < S_{X_1}/S_{X_2} < 2$). The results are illustrated in Tables 6.4 and 6.5, which have the same format with Table 6.2. According to Table 6.4, distinctly, all t values are greater than critical value 2.002. Alternatively, all p values are extremely small for Experiment 1 to 4. It is an evidence that we reject null hypothesis, and observe highly significance between population means for two models. Indeed, number of platoons with size 5 in centralized model are greater than in decentralized model. It proves the observation in Figure 6.2. Considering the results obtained in Table 6.5, oppositely, all t values for all experiments are negative and within critical value range $\pm$ 2.002 except Experiment 2, which is a little bit less than the lower bound of that range. In other words, we fail to reject null hypothesis for Experiments 1, 3, and 4, and, according to p values, we can conclude population means for centralized and decentralized models do not have significant difference. Nevertheless, there is an exception, Experiment 2, which shows there exists some significant difference but not too much between two population means.

Table 6.4: T-test for platoons with size 5*

Hypothesis: $H_0 : \mu_1 = \mu_2, H_1 : \mu_1 > \mu_2$						
Experiment	Confidence Interval (CI)	α	t	p value	Conclusion	Significance
1	95%	0.025	8.929	0.000	reject H_0	highly significant
2	95%	0.025	2.581	0.006	reject H_0	highly significant
3	95%	0.025	4.220	0.000	reject H_0	highly significant
4	95%	0.025	3.731	0.000	reject H_0	highly significant

* in steady-state, *i.e.*, average over the last two hours

Table 6.5: T-test for platoons with size 4*

Hypothesis: $H_0 : \mu_1 = \mu_2, H_1 : \mu_1 \neq \mu_2$						
Experiment	Confidence Interval (CI)	α	t	p value	Conclusion	Significance
1	95%	0.05	-0.019	0.985	fail to reject H_0	not significant
2	95%	0.05	-2.146	0.036	reject H_0	significant
3	95%	0.05	-0.969	0.336	fail to reject H_0	not significant
4	95%	0.05	-0.333	0.740	fail to reject H_0	not significant

* in steady-state, *i.e.*, average over the last two hours

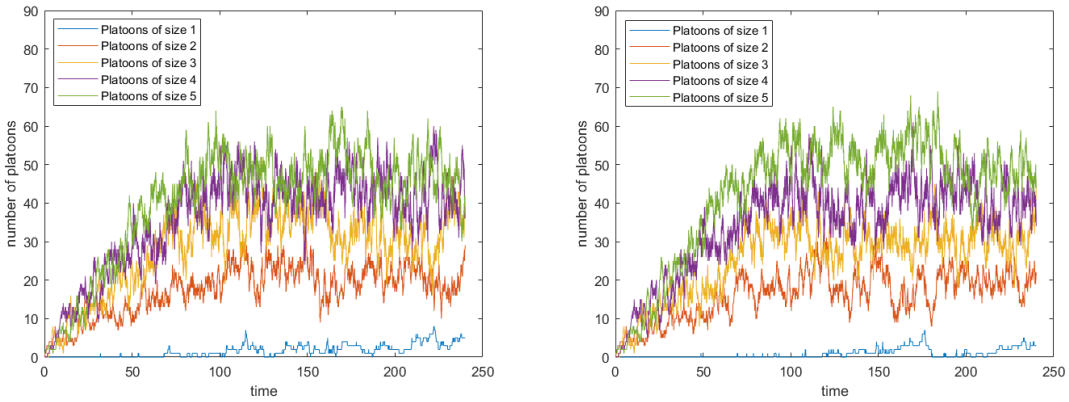

Figure 6.2: Number of platoons by size for Experiment 2 with Decentralized (left) and Centralized (right) model

6.1.2 Energy comparison

Tables 6.6, 6.7, 6.8, and 6.9 report energy results for both centralized and decentralized model. Similarly, Tables 6.6, 6.7, 6.8, and 6.9 have same column formats with Table 4.7. Columns 2, 3, and 4

Table 6.6: Comparison between Decentralized and Centralized Model of Experiment pair (1,5)

Experiment 1 and 5	**Total Energy**			**Acceleration Energy**	**Percentage in Platoon**	
	Low C_D	Average C_D	High C_D		**Mileage**	**Time**
1 (Decentralized)	351,023	388,616	445,004	70,960	41%	43%
1 (Centralized)	344,524	382,095	438,452	64,483	42%	45%
Difference	6,499	6,521	6,553	6,477	-2%	-2%
5	349,417	392,632	457,453	42,276	9%	10%
1 vs. 5 (Decentralized)	-0.46%	1.02%	2.72%	-67.85%	454%	440%
1 vs. 5 (Centralized)	1.40%	2.68%	4.15%	-52.53%	475%	460%

* in steady-state, *i.e.*, average over the last two hours

Table 6.7: Comparison between Decentralized and Centralized Model of Experiment pair (2,6)

Experiment 2 and 6	**Total Energy**			**Acceleration Energy**	**Percentage in Platoon**	
	Low C_D	Average C_D	High C_D		**Mileage**	**Time**
2 (Decentralized)	350,698	389,337	447,297	65,633	43%	43%
2 (Centralized)	348,591	387,255	445,251	63,436	42%	43%
Difference	2,107	2,082	2,046	2,197	1%	1%
6	350,101	393,556	458,738	41,807	9%	9%
2 vs. 6 (Decentralized)	-0.17%	1.07%	2.49%	-56.99%	476%	468%
2 vs. 6 (Centralized)	0.43%	1.60%	2.94%	-51.74%	466%	460%

* in steady-state, *i.e.*, average over the last two hours

present energy results with different drag coefficients. Meanwhile, columns 5, 6, and 7 provide energy results of acceleration and proportion of mileage and time in platoons. Row organization in these tables is different. In Tables 6.6, 6.7, 6.8, and 6.9, we concentrate on comparing results for over the last two hours (*i.e.* in steady-state). Hence, row 2 and 3 show the results respectively for experiments with decentralized and centralized model. Row 4 provides the difference between two types of model. Moreover, row 5 shows the result of reference experiment, where forming new platoons is prohibited. Row 6 and 7 calculate the percentage of energy savings for decentralized and centralized model.

Table 6.6 shows the comparison between decentralized and centralized model of Experiment pair (1,5). The energy savings results of centralized model here yield to the best savings in our experiments owe to more potential platooning opportunities and optimal platooning matching. By contrast to our decentralized model, energy consumption of centralized model based on acceleration is much smaller. With similar percentage of vehicles in platoons, energy consumed by acceleration dominates total energy savings. For example, centralized model consumes 6553 kWh and 6477 kWh respectively in total under high C_D and acceleration less than decentralized model. In other words, if energy consumption from acceleration reduces,

Table 6.8: Comparison between Decentralized and Centralized Model of Experiment pair (3,7)

Experiment 3 and 7	**Total Energy**			**Acceleration Energy**	**Percentage in Platoon**	
	Low C_D	Average C_D	High C_D		**Mileage**	**Time**
3 (Decentralized)	223,639	249,260	287,691	35,038	36%	38%
3 (Centralized)	222,987	248,381	286,472	35,486	37%	39%
Difference	651	878	1,219	-448	-1%	-1%
7	226,578	255,078	297,828	24,107	9%	10%
3 vs. 7 (Decentralized)	1.30%	2.28%	3.40%	-45.35%	393%	386%
3 vs. 7 (Centralized)	1.58%	2.63%	3.81%	-47.21%	401%	397%

* in steady-state, *i.e.*, average over the last two hours

Table 6.9: Comparison between Decentralized and Centralized Model of Experiment pair (4,8)

Experiment 4 and 8	**Total Energy**			**Acceleration Energy**	**Percentage in Platoon**	
	Low C_D	Average C_D	High C_D		**Mileage**	**Time**
4 (Decentralized)	224,028	250,615	290,494	30,772	34%	35%
4 (Centralized)	223,171	249,573	289,177	30,835	35%	36%
Difference	857	1,041	1,318	-63	-1%	-1%
8	226,817	255,476	298,464	23,588	9%	9%
4 vs. 8 (Decentralized)	1.23%	1.90%	2.67%	-30.46%	372%	369%
4 vs. 8 (Centralized)	1.61%	2.31%	3.11%	-30.72%	381%	379%

* in steady-state, *i.e.*, average over the last two hours

decentralized model could lead to better savings. Table 6.7 shows similar situation. However, there only exists a 2100 kWh gap between decentralized and centralized model. As shown in Table 4.2, Experiments 1 and 2 have larger vehicle and platoon input rate, and the only difference between 1 and 2 is platoon speed in Lane 2. Therefore, the primary reason causing large different energy consumption of acceleration is that low speed on Lane 2 can result in locally blocking and congestion. Thus, the platooning decisions made by decentralized model generate more joining and leaving processes.

On the other hand, Tables 6.8 and Table 6.9 provide comparison of Experiment pairs (3,7) and (4,8). Results shown in Table 6.8 and Table 6.9 differ from in Table 6.6 and 6.7. In other words, energy coming from acceleration is not a main factor which affects total energy consumed. For instance, decentralized model consumes 448 kWh less energy from acceleration than centralized model in Experiment 3. Oppositely, decentralized model consumes 1219 kWh more total energy than centralized model. Similar situation appears in Experiment 4. Since Experiments 3 and 4 have less vehicle and platoon input rate, smoother traffic flow can be one reason that there is minor difference for energy from acceleration. Another reason is that decentralized model and centralized model have similar amount of platoons during the simulation. Hence, the primary reason that centralized model saving more in total energy is the better structures of platoons. Namely, a platoon formed by centralized model offering better savings for the entire platoon other than individual. For example, platoons with 5 vehicles are more in centralized model comparing in decentralized model. On account of these reasons, we see there definitely exists a valuable improvement for centralized model.

6.2 Conclusions and Summary

In this study, we developed and evaluated three models: a platoon formation optimization model, a traffic microsimulation model, and an energy prediction model. With their combination, a simulation-optimization framework is established. The optimization model divides the freeway link into platooning zones, then within each zone, determines whether or not each single vehicle should join a specific platoon. Two types of optimization model are built and analyzed in this paper. One is a centralized formulation. Decisions determined by centralized approach is based on the destination of each vehicle as well as the estimated energy savings at the macro level. The other type is a decentralized model. Oppositely, decisions made by decentralized approach concentrate on self payoffs of individual vehicles under competition. The experimental results indicate that considering the destinations in the vehicle-to-platoon assignment decisions leads to a lower total energy savings for the single freeway network. In addition, results in consideration of

self profits also lead to some energy savings. With a comparison conducted, evaluation shows that centralized model offers better platoons composition and system-wide energy savings.

On the other hand, the microsimulation model takes the vehicle-to-platoon assignments as input and simulates the movement and behaviour of each platoon and each vehicle using Vissim's car-following model to provide realistic traffic flow and conditions. Some information is recorded such as location, speed, and destination of each vehicle from the simulation model and utilized as input to the optimization model every 20 seconds. This iterative process continues for four hours. From observations, it takes two hours before steady-state is reached. Thus, our conclusions are mostly drawn from observations over the last two simulation hours (*i.e.*, in steady-state). Our numerical experiment results indicate that savings are maximized if focus lies on forming as many as platoons as possible, as well as on forming longer platoons.

Every 0.5 seconds, detailed vehicle and platooning states are collected from the simulation model which are subsequently processed utilizing the developed prediction model to determine the energy consumed by each vehicle. Before employing the prediction model for energy consumption estimations, we validated its accuracy through the use of a regression model. The results were encouraging as we were able to demonstrate a significantly improved fit of our prediction model to empirical data in comparison to other models proposed in the literature. In particular, our analytical prediction model can accurately reproduce empirical results for short inter-vehicle distances where other existing models fail. The results, which obtained from observing one single platoon, also prove the perfectly matching to the empirical data. Furthermore, we included the additional energy required to form and maintain platoons in our assessment which has not been performed in any of the previous studies. Therefore, a key contribution of this work is the developed energy prediction model which is more applicable to real traffic systems and its reported energy savings are much more realistic compared to previous studies.

6.3 Future Work

In this study, we limited the platoon size to a maximum of five vehicles, but as part of our future work, we plan to study the impact of platoon size on energy savings as well as the impact of platoon speed and associated surrounding traffic conditions. In future work, we will allow single vehicles to join any platoon within the platooning zone instead of only considering those platoons currently behind the vehicles. This study considered a network consisting of only freeway segment. In future work, we plan to extend the analysis to include a network consisting of interstates and non-interstate national highway system routes

to better quantify the potential energy savings with platooning at the regional/state level. In terms of our dynamic game model, we would like to improve our game model based on following criteria. We could add some preference for players in order to affect their respond strategies. Furthermore, we may consider cooperation between single vehicles instead of just competition.

Appendices

Appendix A Other Tables

Table 10: Number of Vehicles in the System

Experiment	Single Vehicles			Vehicles in Platoons		
	Avg†	Std‡	%	Avg	Std	%
1	768	32	59	530	18	41
2	780	32	61	497	17	39
3	542	20	64	304	16	36
4	547	35	66	281	24	34
5	756	33	58	546	16	42
6	788	34	61	497	18	39
7	539	23	64	308	11	36
8	540	30	65	288	21	35
9	726	35	55	582	15	45
10	734	39	57	547	24	43
11	519	23	61	332	14	39
12	532	27	64	297	18	36
13	1115	37	90	119	14	10
14	1114	37	91	114	14	9
15	732	26	90	80	7	10
16	732	26	91	76	7	9

† denotes the average number of vehicles in steady-state, *i.e.*, the last two hours

‡ denotes the corresponding standard deviation

Table 11: Number and Distribution of Vehicles by Platoon Size

Experiment	Size 5			Size 4			Size 3			Size 2		
	Avg†	Std‡	%	Avg	Std	%	Avg	Std	%	Avg	Std	%
1	246	25	46	159	22	30	88	15	17	36	9	7
2	228	28	46	146	23	30	84	15	17	37	10	7
3	132	19	43	91	18	30	57	10	19	24	6	8
4	112	21	40	86	16	31	58	11	21	24	6	8
5	259	24	48	165	21	30	86	13	16	35	8	6
6	224	29	45	147	22	30	83	14	17	40	10	8
7	136	19	44	93	15	30	56	10	18	23	6	8
8	119	19	41	86	16	30	59	12	21	24	7	8
9	283	24	49	173	23	30	90	13	15	35	7	6
10	255	30	47	162	22	30	90	13	16	38	8	7
11	150	23	45	99	16	30	60	11	18	24	5	7
12	125	22	42	88	18	30	59	12	20	25	6	8
13	18	8	15	26	11	21	35	9	29	41	6	35
14	17	8	15	25	11	21	33	8	29	39	6	35
15	12	7	15	15	7	19	21	7	26	32	7	40
16	11	7	15	15	7	19	20	6	26	30	6	40

† denotes the average number of vehicles in a platoon of specific size in steady-state, *i.e.*, the last two hours

‡ denotes the corresponding standard deviation

Table 12: Number and Distribution of Platoons by Size

Experiment	Size 5			Size 4			Size 3			Size 2		
	Avg†	Std‡	%	Avg	Std	%	Avg	Std	%	Avg	Std	%
1	49	5	36	40	6	29	29	5	22	18	5	13
2	46	6	35	37	6	28	28	5	22	19	5	15
3	26	4	33	23	4	28	19	3	24	12	3	15
4	22	4	30	22	4	28	19	4	26	12	3	16
5	52	5	37	41	5	30	29	5	21	17	4	12
6	45	6	34	37	6	28	28	5	21	21	5	17
7	27	4	34	23	4	29	19	3	23	12	3	14
8	24	4	31	22	4	28	20	4	26	12	3	15
9	57	5	39	43	6	29	30	4	20	18	4	12
10	51	6	36	41	5	29	30	4	21	19	4	13
11	30	5	35	25	4	28	20	4	23	12	3	14
12	25	4	32	22	5	28	20	4	25	12	3	15
13	4	2	8	7	3	15	12	3	27	20	3	49
14	3	2	8	6	3	15	11	3	27	20	3	49
15	2	1	8	4	2	13	7	2	24	16	3	54
16	2	1	8	4	2	13	7	2	24	15	3	54

† denotes the average number of platoons of specific size in steady-state, *i.e.*, the last two hours

‡ denotes the corresponding standard deviation

Table 13: Number and Distribution of Vehicles by Position in Platoon

Experiment	Position														
	1			2			3			4			5		
	Avg†	Std‡	%	Avg	Std	%	Avg	Std	%	Avg	Std	%	Avg	Std	%
1	137	4	26	136	4	26	118	5	22	89	6	17	49	5	9
2	131	3	26	129	3	26	110	5	22	82	7	17	46	6	9
3	80	4	26	80	4	26	68	4	23	49	5	16	26	4	9
4	76	6	27	75	6	27	63	6	22	44	5	16	22	4	8
5	140	3	26	139	3	26	122	5	22	93	6	17	52	5	9
6	132	3	27	129	4	26	109	5	22	82	6	16	45	6	9
7	81	2	26	81	2	26	69	3	23	50	4	16	27	4	9
8	77	5	27	77	5	27	65	5	22	45	5	16	24	4	8
9	148	3	26	147	3	25	130	4	22	100	5	17	57	5	10
10	142	5	26	140	5	26	122	6	22	92	6	17	51	6	9
11	87	3	26	87	3	26	74	4	23	55	4	16	30	5	9
12	79	4	27	70	4	27	67	5	22	47	5	16	25	4	8
13	42	4	35	42	4	35	22	4	18	10	3	9	4	2	3
14	40	4	35	40	4	35	21	4	18	10	3	9	3	2	3
15	29	3	36	29	3	36	13	2	17	6	2	8	2	1	3
16	28	3	36	28	3	36	13	2	17	6	2	8	2	1	3

† denotes the average number of vehicles in a specific position in a platoon in steady-state, *i.e.*, the last two hours

‡ denotes the corresponding standard deviation

Table 14: Energy Consumption for the Last Two Hours

Experiment	Total Energy (kWh)			Acceleration Energy	Time in Platoon
	Low C_D	Avg C_D	High C_D		
1	345,891	384,079	441,361	62,986	41%
2	350,444	389,688	448,554	62,329	39%
3	223,024	248,798	287,458	33,662	36%
4	223,884	250,468	290,345	30,651	34%
5	344,958	382,932	439,893	62,987	42%
6	353,310	392,167	450,451	67,225	39%
7	222,905	248,612	287,171	33,905	36%
8	223,366	249,907	289,719	30,324	35%
9	344,524	382,095	438,452	64,483	45%
10	348,591	387,255	445,251	63,436	43%
11	222,987	248,381	286,472	35,486	39%
12	223,171	249,573	289,177	30,835	36%
13	349,417	392,632	457,453	42,276	10%
14	350,101	393,556	458,738	41,807	9%
15	226,578	255,078	297,828	24,107	10%
16	226,817	255,476	298,464	23,588	9%

Table 15: Energy Consumption for all Four Hours

Experiment	Total Energy (kWh)			Acceleration Energy	Time in Platoon
	Low C_D	Avg C_D	High C_D		
1	654,479	728,035	838,367	113,023	37%
2	663,465	738,725	851,616	113,568	35%
3	427,595	477,644	552,717	62,205	32%
4	429,399	480,884	558,110	56,985	30%
5	653,183	726,309	835,999	113,789	38%
6	665,806	740,600	852,793	118,316	36%
7	427,440	477,425	552,403	62,384	32%
8	428,816	480,245	557,388	56,659	31%
9	652,872	725,327	834,008	116,806	40%
10	657,987	732,630	844,595	111,264	39%
11	427,172	476,796	551,232	63,909	34%
12	428,154	479,323	556,076	57,307	32%
13	662,594	744,433	867,192	80,809	10%
14	664,097	746,416	869,895	79,951	10%
15	433,574	488,145	570,001	46,184	10%
16	434,117	489,007	571,341	45,166	9%

Table 16: Energy Consumption of Observed Single Platoon with Different Headway

Experiment	Position	Energy from Aerodynamic Drag			Acceleration	Rolling Friction	Total Energy		
		Low C_D	Average C_D	High C_D			Low C_D	Average C_D	High C_D
0.5s	1	111	134	169	5	62	179	202	237
	2	95	115	145	6	62	163	183	213
	3	91	110	138	8	62	161	180	208
	4	88	106	133	17	62	167	185	212
0.6s	1	111	134	169	5	62	179	202	237
	2	96	116	146	5	62	163	183	213
	3	91	110	139	6	62	160	179	208
	4	88	106	133	15	62	165	183	210
0.7s Base Value	1	111	134	169	5	62	179	202	237
	2	96	117	147	5	62	164	184	214
	3	92	111	140	6	62	161	180	208
	4	88	106	134	17	62	167	185	213
0.8s	1	111	134	169	5	62	179	202	236
	2	97	117	148	6	62	165	185	216
	3	92	112	140	6	62	161	180	209
	4	88	107	134	15	62	166	184	212
0.9s	1	111	134	169	6	62	179	202	237
	2	98	118	149	6	62	166	186	217
	3	93	112	141	6	62	161	181	210
	4	88	107	134	16	62	167	186	213
1.0s	1	111	134	169	6	62	179	202	237
	2	98	119	149	6	62	167	187	218
	3	93	113	142	6	62	162	181	210
	4	89	107	135	16	62	167	186	213

Table 17: Energy Consumption of Observed Single Platoon with Different Speed

Experiment	Position	Energy from Aerodynamic Drag			Acceleration	Rolling Friction	Total Energy		
		Low C_D	Average C_D	High C_D			Low C_D	Average C_D	High C_D
55mph	1	94	113	142	2	62	158	177	206
	2	81	98	123	3	62	146	163	188
	3	77	93	117	3	62	142	158	182
	4	74	90	113	6	62	142	157	180
57.5mph	1	102	123	154	14	62	178	199	231
	2	89	108	135	16	62	167	185	213
	3	86	104	130	17	62	165	183	209
	4	82	99	125	29	62	173	190	216
60mph Base Value	1	111	134	169	5	62	179	202	237
	2	96	117	147	5	62	164	184	214
	3	92	111	140	6	62	161	180	208
	4	88	106	134	17	62	167	185	213
62.5mph	1	120	145	182	11	62	193	218	255
	2	105	126	159	11	62	178	200	232
	3	100	120	151	10	62	172	193	224
	4	95	115	145	29	62	187	206	236
65mph	1	128	155	195	20	62	210	237	277
	2	113	137	172	18	62	193	217	252
	3	109	132	166	14	62	185	208	242
	4	105	127	159	77	62	245	266	299

Table 18: Energy Consumption of Observed Single Platoon with Different Platoon Size

Experiment	Position	Energy from Aerodynamic Drag			Acceleration	Rolling Friction	Total Energy		
		Low C_D	Average C_D	High C_D			Low C_D	Average C_D	High C_D
Size 2	1	111	134	168	6	62	179	202	237
	2	106	128	161	13	62	182	204	237
Size 3	1	112	135	170	1	62	175	198	233
	2	97	117	147	3	62	162	182	212
	3	93	112	141	8	62	163	182	211
Size 4 Base Value	1	111	134	169	5	62	179	202	237
	2	96	117	147	5	62	164	184	214
	3	92	111	140	6	62	161	180	208
	4	88	106	134	17	62	167	185	213
Size 5	1	111	134	169	3	62	177	200	235
	2	96	116	146	6	62	164	184	214
	3	92	111	139	6	62	160	179	207
	4	87	106	133	6	62	155	173	201
	5	84	101	127	15	62	161	178	204
Size 6	1	111	134	168	9	62	182	205	239
	2	97	117	147	10	62	169	189	219
	3	92	111	140	15	62	169	188	217
	4	89	107	135	12	62	163	181	209
	5	85	103	130	13	62	160	178	205
	6	82	99	124	26	62	170	187	212
Size 7	1	111	134	169	9	62	183	206	240
	2	96	116	146	12	62	171	191	221
	3	92	111	139	12	62	166	185	213
	4	88	106	133	21	62	171	189	217
	5	84	102	128	13	62	160	177	203
	6	80	97	122	12	62	155	171	196
	7	77	93	117	28	62	167	183	207

Appendix B Other Figures

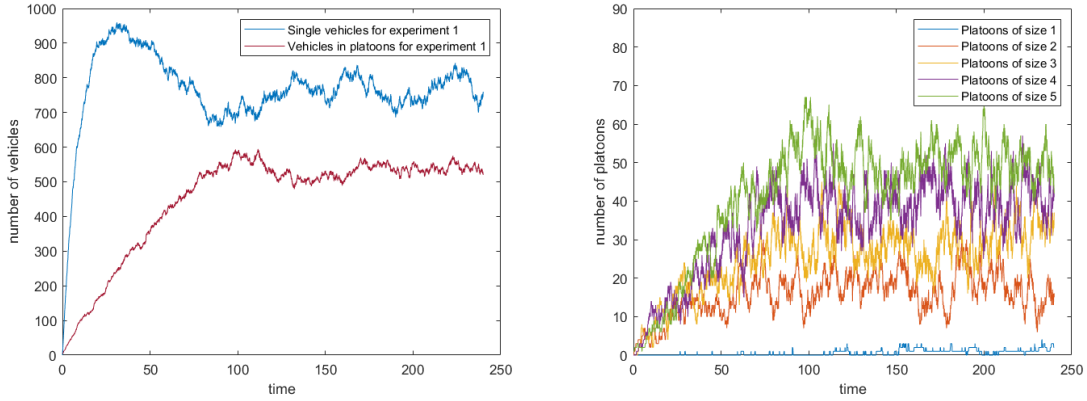

Figure 3: Number of vehicles (left) and number of platoons by size (right) for Experiment 1 (Centralized)

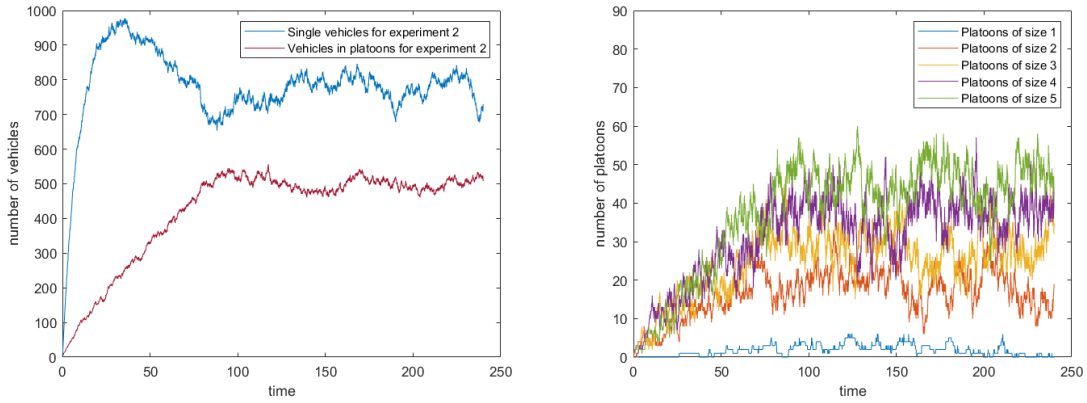

Figure 4: Number of vehicles (left) and number of platoons by size (right) for Experiment 2 (Centralized)

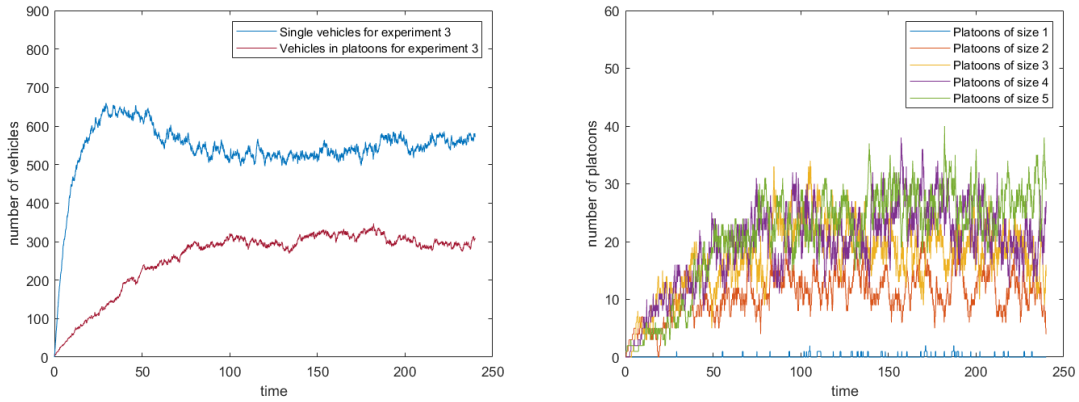

Figure 5: Number of vehicles (left) and number of platoons by size (right) for Experiment 3 (Centralized)

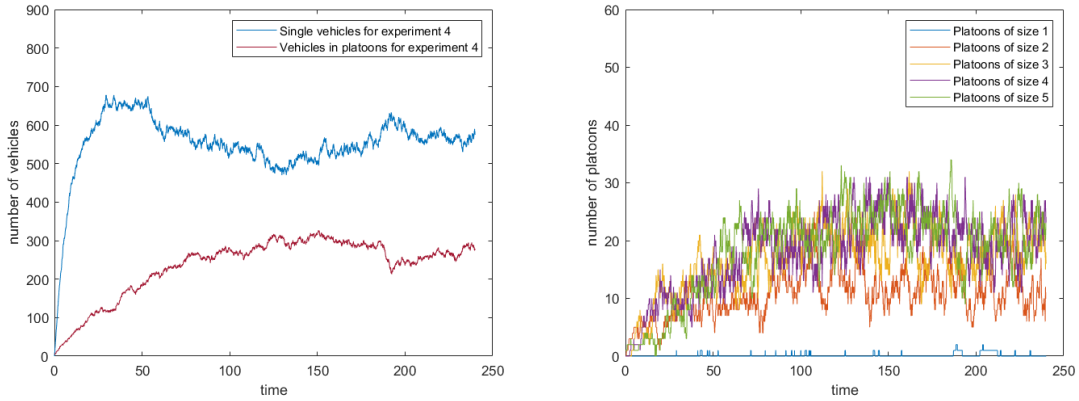

Figure 6: Number of vehicles (left) and number of platoons by size (right) for Experiment 4 (Centralized)

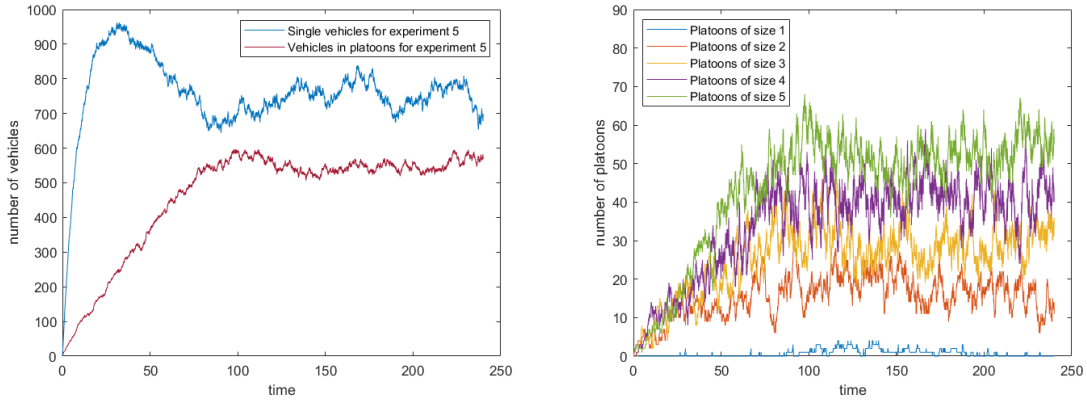

Figure 7: Number of vehicles (left) and number of platoons by size (right) for Experiment 5 (Centralized)

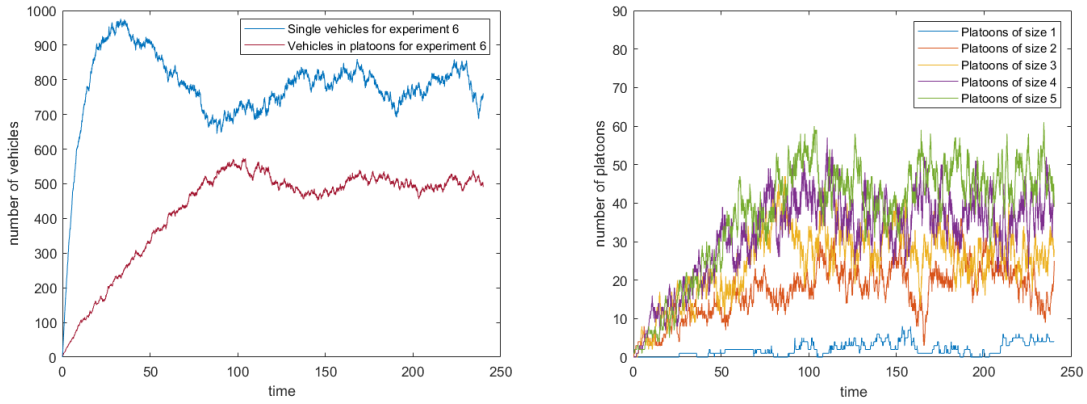

Figure 8: Number of vehicles (left) and number of platoons by size (right) for Experiment 6 (Centralized)

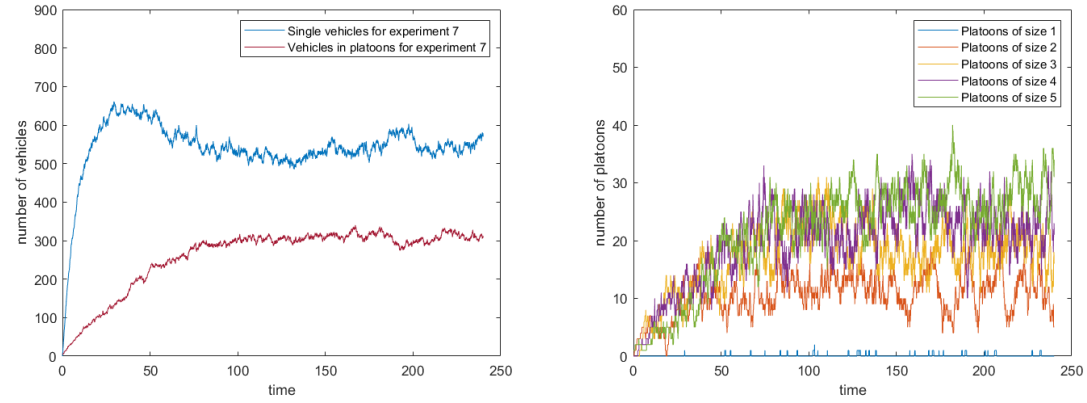

Figure 9: Number of vehicles (left) and number of platoons by size (right) for Experiment 7 (Centralized)

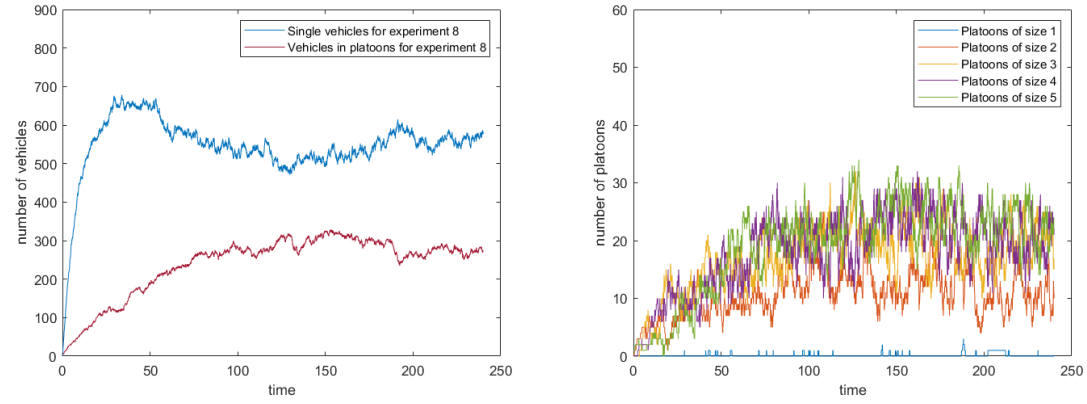

Figure 10: Number of vehicles (left) and number of platoons by size (right) for Experiment 8 (Centralized)

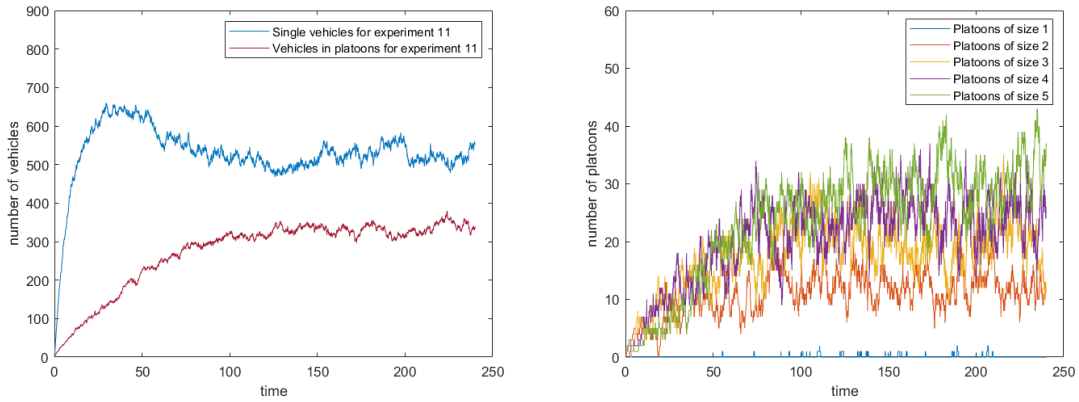

Figure 11: Number of vehicles (left) and number of platoons by size (right) for Experiment 11 (Centralized)

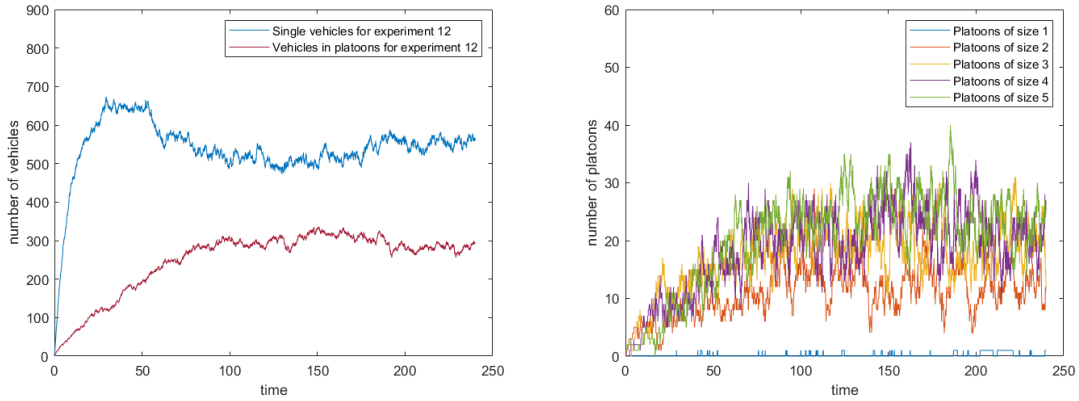

Figure 12: Number of vehicles (left) and number of platoons by size (right) for Experiment 12 (Centralized)

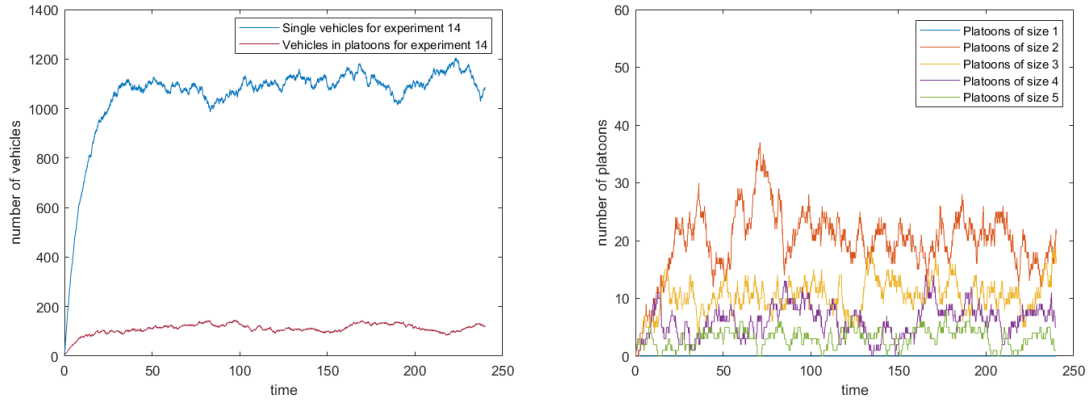

Figure 13: Number of vehicles (left) and number of platoons by size (right) for Experiment 14 or 6 (Centralized or Decentralized)

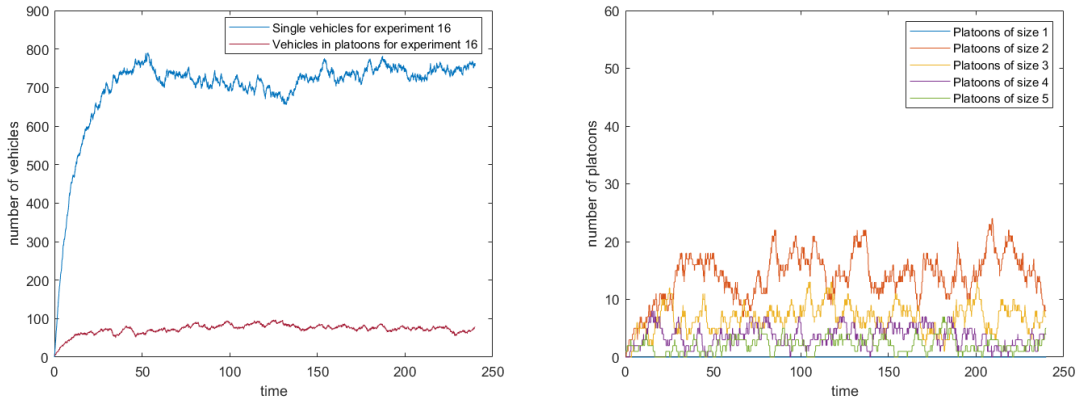

Figure 14: Number of vehicles (left) and number of platoons by size (right) for Experiment 16 or 8 (Centralized or Decentralized)

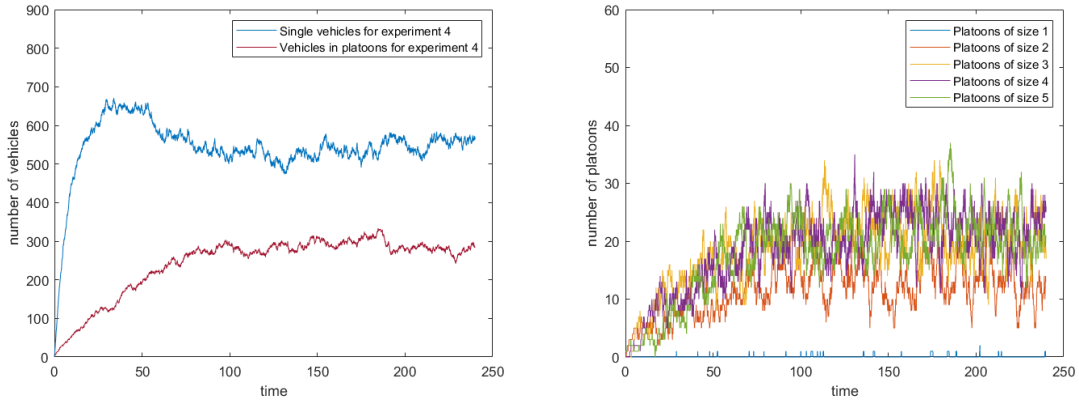

Figure 15: Number of vehicles (left) and number of platoons by size (right) for Experiment 4 (Decentralized)

Bibliography

[1] B. McAuliffe, M. Lammert, X.-Y. Lu, S. Shladover, M.-D. Surcel, and A. Kailas, "Influences on energy savings of heavy trucks using cooperative adaptive cruise control," SAE Technical Paper, Tech. Rep., 2018.

[2] C. Bonnet and H. Fritz, "Fuel consumption reduction in a platoon: Experimental results with two electronically coupled trucks at close spacing," SAE Technical Paper, Tech. Rep., 2000.

[3] M. P. Lammert, A. Duran, J. Diez, K. Burton, and A. Nicholson, "Effect of platooning on fuel consumption of class 8 vehicles over a range of speeds, following distances, and mass," *SAE International Journal of Commercial Vehicles*, vol. 7, no. 2014-01-2438, pp. 626–639, 2014.

[4] A. Al Alam, A. Gattami, and K. H. Johansson, "An experimental study on the fuel reduction potential of heavy duty vehicle platooning," in *13th International IEEE Conference on Intelligent Transportation Systems*, IEEE, 2010, pp. 306–311.

[5] M. Muratori, J. Holden, M. Lammert, A. Duran, S. Young, and J. Gonder, "Potentials for platooning in us highway freight transport," National Renewable Energy Lab.(NREL), Golden, CO (United States), Tech. Rep., 2017.

[6] O. Gehring and H. Fritz, "Practical results of a longitudinal control concept for truck platooning with vehicle to vehicle communication," in *Proceedings of Conference on Intelligent Transportation Systems*, IEEE, 1997, pp. 117–122.

[7] H. Fritz, "Electronic tow-bar based platoon control of heavy duty trucks using vehicle-vehicle communication: Practical results of the chauffeur2 project," in *Proc. 11th World Congress on Intelligent Transport Systems, Nagoya, Aichi, Japan, Nov. 2004*, 2004.

[8] R. Kunze, R. Ramakers, K. Henning, and S. Jeschke, "Organization and operation of electronically coupled truck platoons on german motorways," in *Automation, Communication and Cybernetics in Science and Engineering 2009/2010*, Springer, 2011, pp. 427–439.

[9] S. Tsugawa, "Results and issues of an automated truck platoon within the energy its project," in *2014 IEEE Intelligent Vehicles Symposium Proceedings*, IEEE, 2014, pp. 642–647.

[10] X.-Y. Lu and S. E. Shladover, "Automated truck platoon control," 2011.

[11] F. Browand, J. McArthur, and C. Radovich, "Fuel saving achieved in the field test of two tandem trucks," 2004.

[12] S. Tsugawa, "An overview on an automated truck platoon within the energy its project," *IFAC Proceedings Volumes*, vol. 46, no. 21, pp. 41–46, 2013.

[13] A. Alam, B. Besselink, V. Turri, J. Martensson, and K. H. Johansson, "Heavy-duty vehicle platooning for sustainable freight transportation: A cooperative method to enhance safety and efficiency," *IEEE Control Systems Magazine*, vol. 35, no. 6, pp. 34–56, 2015.

[14] M. Barth, F. An, J. Norbeck, and M. Ross, "Modal emissions modeling: A physical approach," *Transportation Research Record*, vol. 1520, no. 1, pp. 81–88, 1996.

[15] H. Rakha, K. Ahn, and A. Trani, "Development of vt-micro model for estimating hot stabilized light duty vehicle and truck emissions," *Transportation Research Part D: Transport and Environment*, vol. 9, no. 1, pp. 49–74, 2004.

[16] A. Brooker, J. Gonder, L. Wang, E. Wood, S. Lopp, and L. Ramroth, "Fastsim: A model to estimate vehicle efficiency, cost and performance," SAE Technical Paper, Tech. Rep., 2015.

[17] S. Halbach, P. Sharer, S. Pagerit, A. P. Rousseau, and C. Folkerts, "Model architecture, methods, and interfaces for efficient math-based design and simulation of automotive control systems," SAE Technical Paper, Tech. Rep., 2010.

[18] A. Rousseau, S. Halbach, L. Michaels, N. Shidore, N. Kim, N. Kim, D. Karbowski, and M. Kropinski, "Electric drive vehicle development and evaluation using system simulation," *IFAC Proceedings Volumes*, vol. 47, no. 3, pp. 7886–7891, 2014.

[19] B. Lane, B. Shaffer, and G. S. Samuelsen, "Plug-in fuel cell electric vehicles: A california case study," *International Journal of Hydrogen Energy*, vol. 42, no. 20, pp. 14 294–14 300, 2017.

[20] K. Tadakuma, T. Doi, M. Shida, and K. Maeda, "Prediction formula of aerodynamic drag reduction in multiple-vehicle platooning based on wake analysis and on-road experiments," *SAE International Journal of Passenger Cars-Mechanical Systems*, vol. 9, no. 2016-01-1596, pp. 645–656, 2016.

[21] S. Tsugawa, S. Kato, and K. Aoki, "An automated truck platoon for energy saving," in *2011 IEEE/RSJ International Conference on Intelligent Robots and Systems*, IEEE, 2011, pp. 4109–4114.

[22] Q. Deng, "A general simulation framework for modeling and analysis of heavy-duty vehicle platooning," *IEEE Transactions on Intelligent Transportation Systems*, vol. 17, no. 11, pp. 3252–3262, 2016.

[23] I. Johansson, "Simulation studies of impact of heavy-duty vehicle platoons on road traffic and fuel consumption," PhD thesis, KTH Royal Institute of Technology, 2018.

[24] J. Heinovski and F. Dressler, "Platoon formation: Optimized car to platoon assignment strategies and protocols," in *2018 IEEE Vehicular Networking Conference (VNC)*, IEEE, 2018, pp. 1–8.

[25] J. Larson, C. Kammer, K.-Y. Liang, and K. H. Johansson, "Coordinated route optimization for heavy-duty vehicle platoons," in *16th International IEEE Conference on Intelligent Transportation Systems (ITSC 2013)*, IEEE, 2013, pp. 1196–1202.

[26] K. Liang, J. Mårtensson, and K. H. Johansson, "Heavy-duty vehicle platoon formation for fuel efficiency," *IEEE Transactions on Intelligent Transportation Systems*, vol. 17, no. 4, pp. 1051–1061, 2016.

[27] T.-S. Dao, J. P. Huissoon, and C. M. Clark, "A strategy for optimisation of cooperative platoon formation," *International journal of vehicle information and communication systems*, vol. 3, no. 1, pp. 28–43, 2013.

[28] T.-S. Dao, C. M. Clark, and J. P. Huissoon, "Distributed platoon assignment and lane selection for traffic flow optimization," in *2008 IEEE Intelligent Vehicles Symposium*, IEEE, 2008, pp. 739–744.

[29] S.-Y. Han, Y.-H. Chen, L. Wang, and A. Abraham, "Decentralized longitudinal tracking control for cooperative adaptive cruise control systems in a platoon," in *2013 IEEE International Conference on Systems, Man, and Cybernetics*, IEEE, 2013.

[30] T. Renzler, M. Stolz, and D. Watzenig, "Decentralized dynamic platooning architecture with v2v communication tested in omnet++," in *8th International Conference on Connected Vehicles and Expo*, 2019.

[31] A. Rupp, M. Stolz, and M. Horn, "Decentralized cooperative merging using sliding mode control," *IFAC-PapersOnLine*, vol. 51, no. 9, pp. 349–354, 2018.

[32] S. D. Kumaravel, A. A. Malikopoulos, and R. Ayyagari, "Decentralized cooperative merging of platoons of connected and automated vehicles at highway on-ramps," *arXiv preprint arXiv:2002.04826*, 2020.

[33] I. Sajjad, R. Sharma, and R. Gerdes, "A game-theoretic approach and evaluation of adversarial vehicular platooning," in *Proceedings of the 1st International Workshop on Safe Control of Connected and Autonomous Vehicles*, 2017, pp. 35–41.

[34] A. Gattami, A. Al Alam, K. H. Johansson, and C. J. Tomlin, "Establishing safety for heavy duty vehicle platooning: A game theoretical approach," *IFAC Proceedings Volumes*, vol. 44, no. 1, pp. 3818–3823, 2011.

[35] F. Farokhi and K. H. Johansson, "A game-theoretic framework for studying truck platooning incentives," in *16th International IEEE Conference on Intelligent Transportation Systems (ITSC 2013)*, IEEE, 2013, pp. 1253–1260.

[36] A. Johansson, E. Nekouei, K. H. Johansson, and J. Mårtensson, "Multi-fleet platoon matching: A game-theoretic approach," in *2018 21st International Conference on Intelligent Transportation Systems (ITSC)*, IEEE, 2018, pp. 2980–2985.

[37] A. Johansson and J. Mårtensson, "Game theoretic models for profit-sharing in multi-fleet platoons," in *2019 IEEE Intelligent Transportation Systems Conference (ITSC)*, IEEE, 2019, pp. 3019–3024.

[38] R. Schmoyer, P. S. Hu, and P. Swank, *Analysis of vehicle classification and truck weight data of the New England states*. Oak Ridge National Laboratory, 1998.

[39] M. Chowdhury, B. Putman, W. Pang, A. Dunning, K. Dey, L. Chen, *et al.*, "Rate of deterioration of bridges and pavements as affected by trucks," South Carolina. Dept. of Transportation, Tech. Rep., 2013.

[40] J. Y. Wong, *Theory of ground vehicles*. John Wiley & Sons, 2008.

[41] S. Zhang, L. Yu, and G. Song, "Emissions characteristics for heavy-duty diesel trucks under different loads based on vehicle-specific power," *Transportation Research Record*, vol. 2627, no. 1, pp. 77–85, 2017.

[42] G. Paterlini, "Rolling resistance validation," Minnesota Department of Transportation, Tech. Rep., Jul. 2015.

[43] S. Tadelis, *Game theory: an introduction*. Princeton university press, 2013.